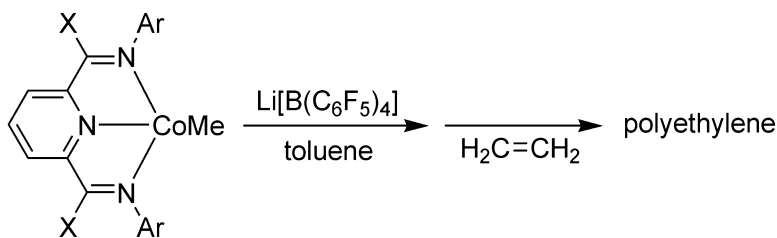


Chelate Bis(imino)pyridine Cobalt Complexes: Synthesis, Reduction, and Evidence for the Generation of Ethene Polymerization Catalysts by Li Cation Activation

Nina Kleigrewe, Winfried Steffen, Tobias Blmker, Gerald Kehr, Roland Frhlich, Birgit Wibbeling, Gerhard Erker, Julia-Christina Wasilke, Guang Wu, and Guillermo C. Bazan

J. Am. Chem. Soc., **2005**, 127 (40), 13955-13968 • DOI: 10.1021/ja052129k • Publication Date (Web): 20 September 2005

Downloaded from <http://pubs.acs.org> on March 25, 2009



(X = Ph, CH₃ or OCH₃, Ar = 2,6-diisopropylphenyl)

More About This Article

Additional resources and features associated with this article are available within the HTML version:

- Supporting Information
- Links to the 11 articles that cite this article, as of the time of this article download
- Access to high resolution figures
- Links to articles and content related to this article
- Copyright permission to reproduce figures and/or text from this article

[View the Full Text HTML](#)

Chelate Bis(imino)pyridine Cobalt Complexes: Synthesis, Reduction, and Evidence for the Generation of Ethene Polymerization Catalysts by Li⁺ Cation Activation

Nina Kleigrewe,[†] Winfried Steffen,[†] Tobias Blömker,[†] Gerald Kehr,[†]
Roland Fröhlich,^{†,§} Birgit Wibbeling,^{†,§} Gerhard Erker,^{*,†} Julia-Christina Wasilke,^{†,‡}
Guang Wu,^{‡,§} and Guillermo C. Bazan^{*,‡}

Contribution from the *Organisch-Chemisches Institut Universität Münster, Corrensstr. 40, D-48149 Münster, Germany*, and *Department of Chemistry and Biochemistry, Institute for Polymers and Organic Solids, University of California, Santa Barbara, CA 93106*

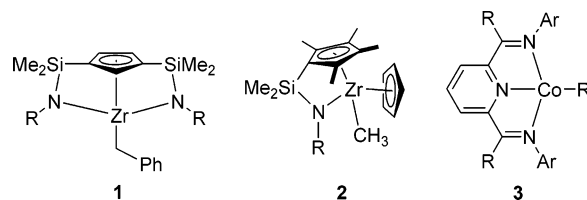
Received April 27, 2005; E-mail: erker@uni-muenster.de; bazan@chem.ucsb.edu

Abstract: Treatment of the bis(iminobenzyl)pyridine chelate Schiff-base ligand **8** (lig^{Ph}) with FeCl₂ or CoCl₂ yielded the corresponding (lig^{Ph})MCl₂ complexes **9** (Fe) and **10** (Co). The reaction of **10** with methyl lithium or "butadiene-magnesium" resulted in reduction to give the corresponding (lig^{Ph})Co(I)Cl product **11**. Similarly, the bis(aryliminoethyl)pyridine ligand (lig^{Me}) was reacted with CoCl₂ to yield (lig^{Me})CoCl₂ (**12**). Reduction to (lig^{Me})CoCl (**13**) was effected by treatment with "butadiene-magnesium". Complex **13** reacted with Li[B(C₆F₅)₄] in toluene followed by treatment with pyridine to yield [(lig^{Me})Co⁺-pyridine] (**15**). The reaction of the Co(II) complexes **10** or **12** with ca. 3 molar equiv of methyl lithium gave the cobalt(I) complexes **16** and **17**, respectively. Treatment of the (lig^{Me})CoCH₃ (**17**) with Li[B(C₆F₅)₄] gave a low activity ethene polymerization catalyst. Likewise, complex **16** produced polyethylene (activity = 33 g(PE) mmol(cat)⁻¹ h⁻¹ bar⁻¹ at room temperature) upon treatment with a stoichiometric amount of Li[B(C₆F₅)₄]. A third ligand (lig^{OMe}) was synthesized featuring methoxy groups in the ligand backbone (**22**). Coordination to FeCl₂ and CoCl₂ yielded the desired compounds **23** and **24**. Reaction with MeLi gave (lig^{OMe})CoMe (**25/26**). Treatment of **25/26** with excess B(C₆F₅)₃ gave the η⁶-arene cation complex **27**, where one Co–N linkage was cleaved. Activation of **25/26** with Li[B(C₆F₅)₄] again gave a catalytically active species.

Introduction

Homogeneous Ziegler–Natta chemistry has seen a variety of advancements in the recent years. After the extensive development of Group 4 bent metallocene-based catalysts^{1,2} other metal complex types have become increasingly important in this chemistry. The bridged Cp/amido complexes of the Group 3 and 4 metals (the "constrained geometry catalysts")³ and several types of chelate complexes of the late transition metals represent noteworthy examples of this important development.⁴ All these systems seem to have in common that the respective alkyl-metal cation systems are generated in the course of the

Scheme 1



activation process and that alkyl-metal cations represent the active stages of the catalyst systems in the repetitive steps of the actual catalytic cycle.¹

A few systems were recently described that seemed to show some deviation from the rule. Royo et al.⁵ observed that the Me₂Si-bridged bis(amido)/Cp zirconium complex (**1**, see Scheme 1) polymerized ethene upon activation. It was assumed that a catalyst was formed that initially did apparently not contain a metal-bound alkyl group. Chen et al.⁶ have recently described a bent metallocene system (**2**) of similar features. He proposed

[†] Universität Münster

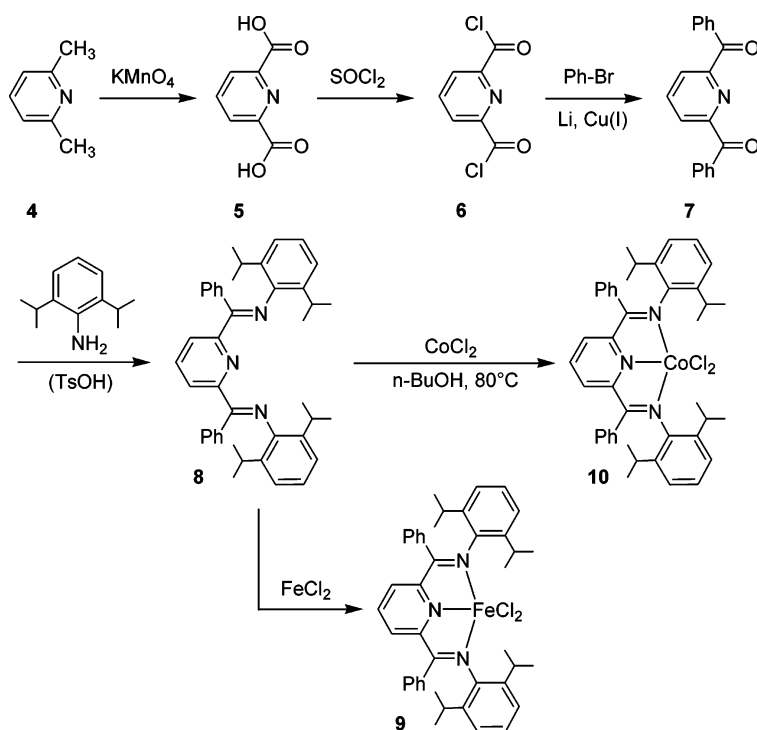
[‡] University of California

[§] Contact this author for information regarding X-ray crystal structure determinations.

- (1) (a) Marks, T. J. *Acc. Chem. Res.* **1992**, *25*, 57–65. (b) Brintzinger, H. H.; Fischer, D.; Müllhaupt, R.; Rieger B.; Waymouth, R. M. *Angew. Chem.* **1995**, *107*, 1255–1283; *Angew. Chem., Int. Ed. Engl.* **1995**, *34*, 1143–1170. (c) Bochmann, M. J. *Chem. Soc., Dalton Trans.* **1996**, 255–270. (d) Kaminsky, W. *J. Chem. Soc., Dalton Trans.* **1998**, 1413–1418.
- (2) (a) Erker, G. *Acc. Chem. Res.* **2001**, *34*, 309–317. (b) Erker, G. *Chem. Commun.* **2003**, 1469–1476.
- (3) Reviews: (a) McKnight, A. L.; Waymouth, R. M. *Chem. Rev.* **1998**, *98*, 2587–2598. (b) Okuda, J.; Eberle, T. Half-Sandwich Complexes as Metallocene Analogues. In *Metallocenes – Synthesis, Reactivity, Applications*; Togni, A., Halterman, R. L., Eds.; Wiley-VCH: Weinheim, 1998; Vol. 1, pp 415–453. See also: (c) Kunz, K.; Erker, G.; Döring, S.; Fröhlich, R.; Kehr, G. *J. Am. Chem. Soc.* **2001**, *123*, 6181–6182. (d) Bredeau, S.; Altenhoff, G.; Kunz, K.; Döring, S.; Grimme, S.; Kehr, G.; Erker, G. *Organometallics* **2004**, *23*, 1836–1844.

- (4) (a) Britovsek, G. J. P.; Gibson, V. C.; Wass, D. F. *Angew. Chem.* **1999**, *111*, 448–468; *Angew. Chem., Int. Ed.* **1999**, *38*, 428–447. (b) Ittel, S. D.; Johnson, L. K.; Brookhart, M. *Chem. Rev.* **2000**, *100*, 1169–1203. (c) Gibson, V. C.; Spitzmesser, S. K. *Chem. Rev.* **2003**, *103*, 283–315.
- (5) Cano, J.; Royo, P.; Lanfranchi, M.; Pellinghelli, M. A.; Tiripicchio, A. *Angew. Chem.* **2001**, *113*, 2563–2565; *Angew. Chem., Int. Ed.* **2001**, *40*, 2495–2497.
- (6) Jin, J.; Wilson, D. R.; Chen, E. Y.-X. *Chem. Commun.* **2002**, 708–709.

Scheme 2



that alkyl transfer from the $[R-Al(C_6F_5)_3]^-$ counteranion to coordinated ethene represented the essential carbon–carbon bond forming step (followed by alkyl transfer from zirconium to aluminum) at such initially seemingly transition metal alkyl-free catalyst systems.

A few chelate bis(iminoalkyl)pyridine cobalt systems were described by Gal *et al.*⁷ and Gibson *et al.*^{8,9} that showed related characteristics. The [bis(iminoalkyl- $\kappa N, N'$)pyridine- κN]Co(II)-Cl₂ complexes reacted with alkyllithium reagents by reduction to yield the corresponding (lig)Co(I)Cl complexes. Subsequent activation with, e.g., methylalumoxane (MAO) gave active ethene polymerization catalysts. Following the commonly accepted activation mechanisms^{10,11} the systems derived from **3** are also homogeneous catalysts that might initially be lacking a metal–carbon σ -bond. Alkyl transfer from an $R-[B]^-$ or

$R-[Al]^-$ -type counteranion could potentially again represent a mode of catalytic action at these special systems.

We have now observed that the (lig)Co(I)CH₃ complexes gave active ethene polymerization catalysts simply by treatment with Li[B(C₆F₅)₄]. This shines some light on the potential olefin polymerization pathways followed at the small group of early or late metal Ziegler–Natta catalyst that operate under such apparently “alkyl-free” conditions. In this paper we will describe the synthesis, some chemical and structural properties of such systems, and their catalytic olefin polymerization properties upon activation with Li⁺ cation.

Results and Discussion

Synthesis of the Metal Complexes. The bis(*N*-aryliminobenzyl)pyridine ligand system (**8**, lig^{Ph}) was prepared analogously as described by Esteruelas *et al.*¹² Pyridine-2,6-dicarboxylic acid **5** was prepared by KMnO₄ oxidation of 2,6-dimethylpyridine. Subsequent conversion to the acid chloride (**6**) followed by phenylcuprate coupling gave **7**, which was converted to the bis(iminobenzyl)pyridine ligand (**8**) by acid-catalyzed condensation with 2,6-diisopropylaniline. The ligand system **8** was treated with iron(II) chloride to yield the paramagnetic chelate complex **9**. Treatment of **8** with CoCl₂ in boiling *n*-butanol eventually gave the paramagnetic [bis(*N*-aryliminobenzyl- $\kappa N, N'$)-pyridine- κN]cobalt(II) dichloride system **10** (72% isolated) (Scheme 2).

- (7) Kooistra, T. M.; Knijnenburg, Q.; Smits, J. M. M.; Horton, A. D.; Budzelaar, P. H. M.; Gal, A. W. *Angew. Chem.* **2001**, *113*, 4855–4858; *Angew. Chem., Int. Ed.* **2001**, *40*, 4719–4722.
- (8) Gibson, V. C.; Humphries, M. J.; Tellmann, K. P.; Wass, D. W.; White, A. J. P.; Williams, D. J. *Chem. Commun.* **2001**, 2252–2253.
- (9) (a) Britovsek, G. J. P.; Bruce, M.; Gibson, V. C.; Kimberley, B. S.; Maddox, P. J.; Mastroianni, S.; McTavish, S. J.; Redshaw, C.; Solan, G. A.; Strömberg, S.; White, A. J. P.; Williams, D. J. *J. Am. Chem. Soc.* **1999**, *121*, 8728–8740. (b) Britovsek, G. J. P.; Gibson, V. C.; Spitzmesser, S. K.; Tellmann, K. P.; White, A. J. P.; Williams, D. J. *J. Chem. Soc., Dalton Trans.* **2002**, 1159–1171. Clentsmith, G. K. B.; Gibson, V. C.; Hitchcock, P. B.; Kimberley, B. S.; Rees, C. W. *Chem. Commun.* **2002**, 1498–1499. Bianchini, C.; Mantovani, G.; Meli, A.; Migliacci, F.; Zanobini, F.; Laschi, F.; Somazzi, A. *Eur. J. Inorg. Chem.* **2003**, 1620–1631. (c) Dias, E. L.; Brookhart, M.; White, P. S. *Organometallics* **2000**, *19*, 4995–5004. Britovsek, G. J. P.; Mastroianni, S.; Solan, G. A.; Baugh, S. P. D.; Redshaw, C.; Gibson, V. C.; White, A. J. P.; Williams, D. J.; Elsegood, M. R. *J. Chem.—Eur. J.* **2000**, *6*, 2221–2231. Britovsek, G. J. P.; Gibson, V. C.; Kimberley, B. S.; Mastroianni, S.; Redshaw, C.; Solan, G. A.; White, A. J. P.; Williams, D. J. *J. Chem. Soc., Dalton Trans.* **2001**, 1639–1644. Gibson, V. C.; Tellmann, K. P.; Humphries, M. J.; Wass, D. F. *Chem. Commun.* **2002**, 2316–2317. Britovsek, G. J. P.; Gibson, V. C.; Hoarau, O. D.; Spitzmesser, S. K.; White, A. J. P.; Williams, D. J. *Inorg. Chem.* **2003**, *42*, 3454–3465. Small, B. L. *Organometallics* **2003**, *22*, 3178–3183. Chen, Y.; Chen, R.; Quian, C.; Dong, X.; Sun, J. *Organometallics* **2003**, *22*, 4312–4321. Tellmann, K. P.; Gibson, V. C.; White, A. J. P.; Williams, D. J. *Organometallics* **2005**, *24*, 280–286. Humphries, M. J.; Tellmann, K. P.; Gibson, V. C.; White, A. J. P.; Williams, D. J. *Organometallics* **2005**, *24*, 2039–2050 and references cited in these recent articles.

- (10) (a) Yang, X.; Stern, C. L.; Marks, T. J. *J. Am. Chem. Soc.* **1991**, *113*, 3623–3625. (b) Chien, J. C. W.; Tsai, W.-M.; Rausch, M. D. *J. Am. Chem. Soc.* **1991**, *113*, 8570–8571. (c) Bochmann, M.; Jaggard, A. J.; Nicholls, J. C. *Angew. Chem.* **1990**, *102*, 830–832; *Angew. Chem., Int. Ed. Engl.* **1990**, *29*, 780–782. (d) Yang, X.; Stern, C. L.; Marks, T. J. *J. Am. Chem. Soc.* **1994**, *116*, 10015–10031. Reviews: (e) Jordan, R. F. *Adv. Organomet. Chem.* **1991**, *32*, 325–387. (f) Sinn, H.; Kaminsky, W. *Adv. Organomet. Chem.* **1980**, *18*, 99–149. (g) Chen, E. Y.-X.; Marks, T. J. *Chem. Rev.* **2000**, *100*, 1391–1434.
- (11) See also: Strauch, J. W.; Erker, G.; Kehr, G.; Fröhlich, R. *Angew. Chem.* **2002**, *114*, 2662–2664; *Angew. Chem., Int. Ed.* **2002**, *41*, 2543–2546.
- (12) Esteruelas, M. A.; López, A. M.; Méndez, L.; Oliván, M.; Oñate, E. *Organometallics* **2003**, *22*, 395–406 and references therein.

The [bis(*N*-aryliminobenzyl- $\kappa N, N'$)pyridine- κN]CoCl₂ complex **10** was reacted with ca. 0.5 molar equiv of “butadiene-magnesium”.¹³ As in the related cases described in the literature,^{7,8} we did not observe the formation of a metal-dialkyl or metal-butadiene¹¹ products. Instead the cobalt(II) complex **10** was reduced to the corresponding cobalt(I) chloride **11**. Complex **11** is diamagnetic. It features the NMR resonances as expected for a complex with C_{2v} symmetry.

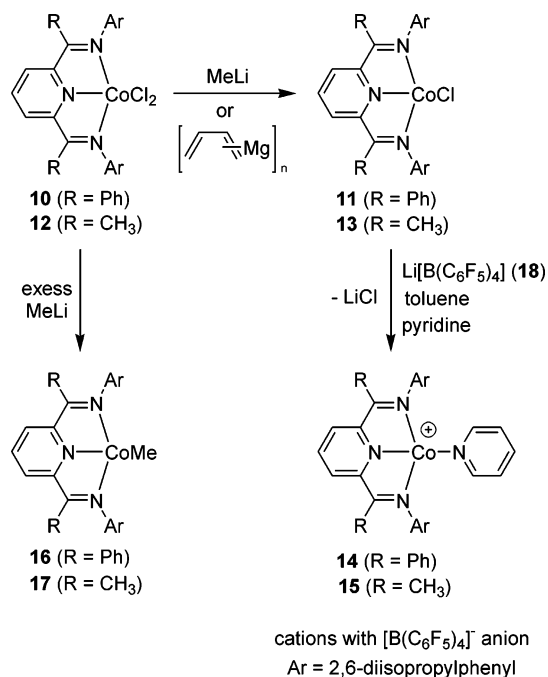
Thus, we have observed ¹H NMR signals at δ 9.53 (t, 1H) and 7.23 (d, 2H) of the central disubstituted pyridine moiety, a single set of phenyl substituent resonances [δ 7.82 (d, 4H), 7.32 (t, 2H), and 7.04 (t, 4H)] in addition to one set of signals of the pair of *N*-(2,6-diisopropylphenyl) substituents [δ 7.46 (t, 2H), 7.25 (d, 4H), and δ 3.66 (sept., 4H), 1.16 (d, 24H, isopropyl)]. The methyl groups of each isopropyl substituent of **11** are diastereotopic [¹³C NMR in *d*₆-benzene at ambient temperature: δ 29.3 (CHMe₂), 24.6 and 23.3 (each CH(CH₃)₂)]. Complex **11** contains a prochiral axis within the =*N*-(2,6-diisopropylphenyl) structural subunit.

The related [bis(*N*-aryliminoethyl- $\kappa N, N'$)pyridine- κN]CoCl₂ complex (**12**, (lig^{Me})CoCl₂) was prepared analogously as described by Gibson et al.^{9a} It was treated with 1 molar equiv of the “butadiene-magnesium” reagent in toluene solution. Quite differently from a series of related chelate bis(imine)nickel(II) dichloride complexes,^{11,14} formation of a stable butadiene complex was not observed. Instead, reduction from (lig^{Me})CoCl₂ to (lig^{Me})CoCl again prevailed, and we isolated the cobalt(I) chloride complex (**13**) in 56% yield. Again diastereotopic splitting of the isopropyl methyl signals is observed in both the ¹H NMR [δ 3.33 (sept., ³J_{HH} = 6.9 Hz, 4H, CHMe₂), δ 1.17 and 1.05 (each d, ³J_{HH} = 6.9 Hz, each 12H, CH(CH₃)₂) and the ¹³C NMR spectrum [δ 29.1 (CHMe₂), 24.0 and 23.8 (CH(CH₃)₂)].

Treatment of the (lig^{Ph})CoCl₂ complex **10** with >2 molar equiv of methyllithium resulted in the formation of the cobalt(I) methyl complex **16**. The Co–CH₃ ¹H NMR resonance of **16** occurs at δ 1.07 (s). Again, the signals of diastereotopic isopropyl methyl groups of the N–C₆H₃(2,6-bis-CHMe₂) units are observed for complex **16** (¹H: 1.05, 0.56 (each d, *J*_{HH} = 6.8 Hz); ¹³C: 22.1, 22.5). The corresponding cobalt(I) methyl complex **17**, previously described by Gal et al.,⁷ was synthesized analogously. In both cases it may safely be assumed that the cobalt(I) chloride complexes **11** and **13**, respectively, may be intermediates of this reaction sequence.

Complex **13** was treated with Li[B(C₆F₅)₄] at room temperature in toluene. This resulted in the abstraction of the chloride ligand from cobalt. Probably, a [(lig^{Me})Co⁺] cation was formed. This was subsequently trapped by the addition of pyridine to the reaction mixture which led to the formation of the [(lig^{Me})Co⁺–pyridine] adduct (**15**, see Scheme 3). Similarly, [(lig^{Ph})Co⁺–pyridine] (**14**) was formed from **11** by treatment with Li[B(C₆F₅)₄] followed by the addition of pyridine.

Scheme 3



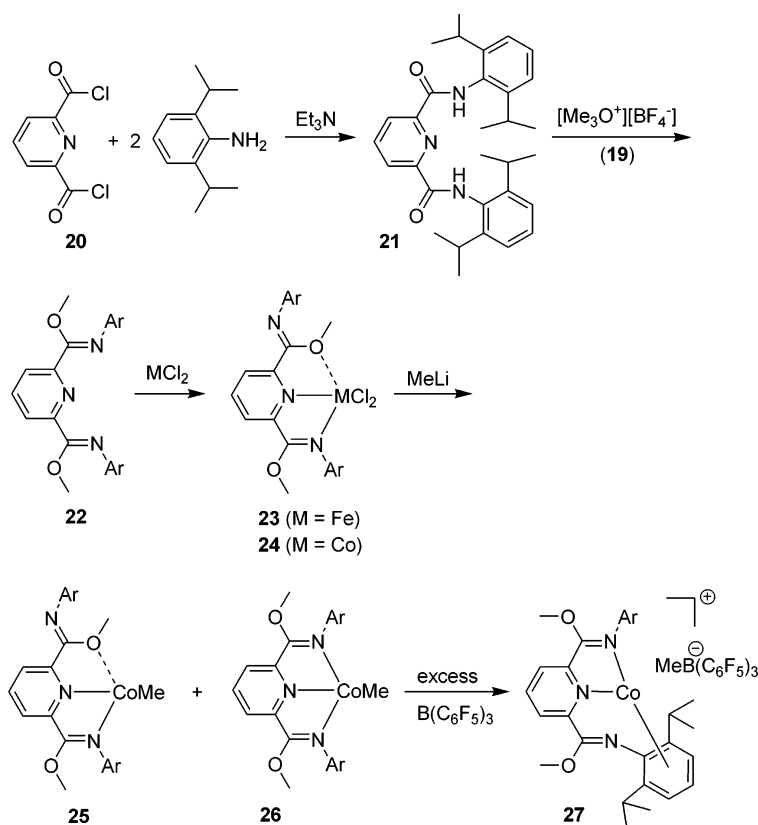
Gibson et al. recently reported the synthesis of the ligand system **22a** (see Scheme 4; Ar = mesityl) and the formation of its *N,N,N*-coordinated FeCl₂ complex.¹⁵ We had prepared the related 2,6-diisopropylphenyl substituted ligand **22** [(lig^{OMe})] by a different route. We treated the pyridine-2,6-diacid chloride (**20**) with 2,6-diisopropylaniline and reacted the resulting carboxylic acid amide (**21**) with Meerwein's reagent [Me₃O⁺][BF₄[−]] (**19**) to obtain **22** (see Scheme 4). Reaction of this ligand (**22**) with iron dichloride gave the iron complex **23** as a light pink powder, which was characterized by elemental analysis and X-ray diffraction. It deserves mentioning here, since crystallization from hot toluene by slowly cooling the solution to room temperature overnight gave single crystals featuring a different coordination mode than the one reported by Gibson et al.¹⁵ (see below). Reaction of **22** with cobalt dichloride was immediate with a color change from blue to green. The product (**24**) was isolated after 1 h of reaction time as a green solid and was characterized by elemental analysis and X-ray diffraction. The reaction of **24** with 1 equiv of methyllithium did not yield the expected^{7,8} 2,6-bis-[(2,6-diisopropylphenyliminomethoxy- $\kappa N, O$)pyridine- κN]cobalt(I) chloride ((lig^{OMe})CoCl), and the only new species detected was methyl-2,6-bis-[(2,6-diisopropylphenyliminomethoxy- $\kappa N, N'$)pyridine- κN]cobalt(I) ((lig^{OMe})CoMe, **26**). The ratio of cobalt complex to methyllithium was increased to 1:2, and the desired methylated Co(I) compound (**26**) was obtained in good yields, sometimes accompanied by a second diamagnetic minor product that was tentatively assigned the structure of the isomer **25** (see Scheme 4). Upon addition of 5 equiv of B(C₆F₅)₃, the purple solution turned blue while the methide is abstracted by B(C₆F₅)₃. This resulted in the formation of a cationic [(lig^{OMe})Co⁺] species (**27**) with a [MeB(C₆F₅)₃][−] counterion.

X-ray Crystal Structure Analyses. Several of the compounds synthesized in the course of this study were characterized

- (13) Yasuda, H.; Kajihara, Y.; Mashima, K.; Nagasuna, K.; Lee, K.; Nakamura, A. *Organometallics* **1982**, *1*, 388–396 and references therein.
(14) See also: (a) Erker, G.; Wicher, J.; Engel, K.; Rosenfeldt, F.; Dietrich, W.; Krüger, C. *J. Am. Chem. Soc.* **1980**, *102*, 6344–6346. (b) Erker, G.; Krüger, C.; Müller, G. *Adv. Organomet. Chem.* **1985**, *24*, 1–39. (c) Yasuda, H.; Tatsumi, K.; Nakamura, A. *Acc. Chem. Res.* **1985**, *18*, 120–126. (d) Dahlmann, M.; Erker, G.; Fröhlich, R.; Meyer, O. *Organometallics* **1999**, *18*, 4459–4461. (e) Erker, G.; Kehr, G.; Fröhlich, R. *Adv. Organomet. Chem.* **2004**, *51*, 109–162.

- (15) (a) Smit, T. M.; Tomov, A. K.; Gibson, V. C.; White, A. J. P.; Williams, D. J. *Inorg. Chem.* **2004**, *43*, 6511–6512. (b) Bennett, A. U.S. Patent Appl. Publ. U.S. 6,423,848 B2, 2002 (E. I. Du Pont De Nemours and Company, USA).

Scheme 4



by X-ray diffraction. First, we investigated the free ligand system **8** by an X-ray crystal structure analysis (see Figure 1 and Table 1). In the solid state this bulky bis(*N*-arylimino)pyridine derivative adopts a conformation that is characterized by a nonplanar arrangement of the two imino substituents at the central pyridine unit. The corresponding dihedral angles N4-C3-C2-N1 ($-67.3(2)^\circ$) and N4-C8-C9-N10 ($-85.5(2)^\circ$) indicate an almost orthogonal orientation of the imino systems relative to the pyridine core. The compound **8** adopts a chiral, close to C_2 -symmetric structure. The $\text{C}=\text{N}$ bonds of the substituents are short (both $1.279(2)$ Å). The planes of the

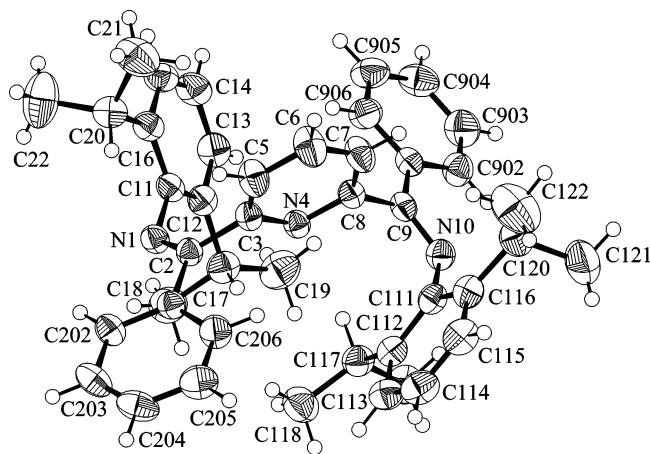


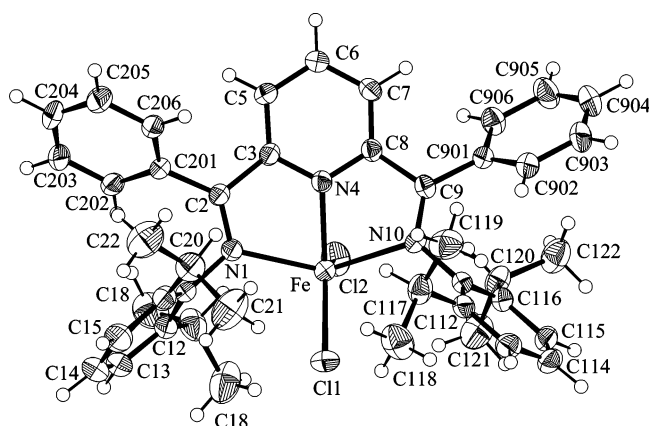
Figure 1. A view of the molecular geometry of the ligand system **8**. Selected bond lengths (Å) and angles (deg): N1-C11 $1.428(2)$, C2-C3 $1.506(2)$, C3-N4 $1.338(2)$, N4-C8 $1.341(2)$, C8-C9 $1.501(2)$, N10-C111 $1.428(2)$; N1-C2-C3 $123.3(1)$, C2-C3-N4 $114.9(1)$, C3-N4-C8 $117.7(1)$, N4-C8-C9 $114.5(1)$, C8-C9-N10 $122.7(1)$. For additional values see Table 1.

adjacent phenyl substituents are oriented such to allow for some π -conjugation with the $\text{C}=\text{N}$ double bond systems (θ C902-C901-C9-N10 $-4.3(2)^\circ$ and C202-C201-C2-N1 $-17.3(2)^\circ$). In contrast, the bulky 2,6-diisopropylphenyl substituents at the imino nitrogen atoms are rotated away from any significant π -interaction (θ C112-C111-N10-C9 $90.2(2)^\circ$ and C12-C11-N1-C2 $99.6(2)^\circ$). It must be noted that in the free ligand **8** the 2,6-diisopropylphenyl substituents are *Z*-oriented with the pyridine moiety at the central $\text{C}=\text{N}$ unit (θ C3-C2-N1-C11 : $-2.7(2)^\circ$, C8-C9-N10-C111 : $0.7(2)^\circ$). Consequently, the phenyl substituents at the imino (sp^2)-carbon center are oriented toward the side of the electron lone pair at the adjacent planar nitrogen center, i.e., *E*-oriented to the respective 7,6-diisopropylphenyl substituent (θ C201-C2-N1-C11 $178.6(1)^\circ$, C901-C9-N10-C111 : $-177.1(1)^\circ$). This is opposite to the structural orientation of these substituents at the $\text{C}=\text{N}$ double bonds in the metal complexes derived from **8**, where this specific configuration would not allow for chelate formation.

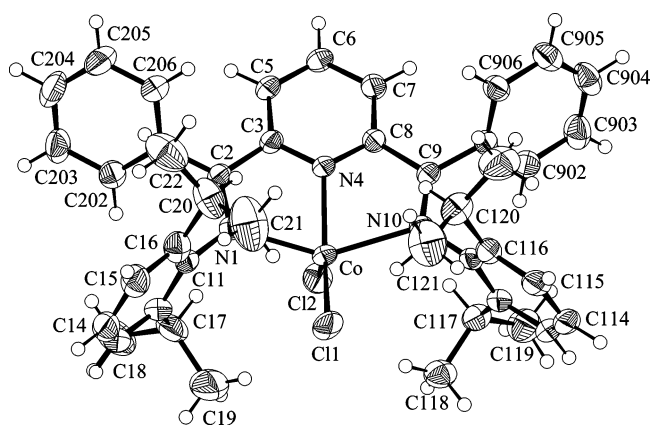
Both imino-nitrogen centers of **8** were inverted¹⁵ to form the paramagnetic chelate [bis(imino)pyridine] MCl_2 complex **9** (Fe) and **10** (Co). In both complexes the metal centers are pentacoordinated,^{9b} featuring a distorted square pyramidal geometry. The three nitrogen atoms from the chelate ligand and one chloride form the base, and the remaining chloride ligand is found in the apical position (see Figures 2 and 3). In the Fe complex **9** the corresponding bond angles at the base amount to $142.34(9)^\circ$ (N1-Fe-N10), $150.69(8)^\circ$ (N4-Fe-C11), $74.64(9)^\circ$ (N1-Fe-N4), $73.16(9)^\circ$ (N4-Fe-N10), $100.27(7)^\circ$ (N10-Fe-C11), and $98.26(7)^\circ$ (C11-Fe-N1). The magnitude of the distortion is illustrated by the values of the bond angles of the chelate ligand nitrogens to the apical chloride ligand:

Table 1. Selected Structural Data of the Chelate Ligand **8** and the Complexes **9–11**, **13**, and **15**

compound	8	9	10	11	13	15
ML _n	-	FeCl ₂	CoCl ₂	CoCl	CoCl	Co(pyr) ⁺
C2–N1	1.279(2)	1.297(4)	1.298(4)	1.321(2)	1.322(3)	1.309(4)
C9–N10	1.279(2)	1.296(4)	1.288(4)	1.329(2)	1.326(3)	1.313(4)
M–N1	-	2.210(2)	2.235(3)	1.914(1)	1.907(2)	1.918(3)
M–N10	-	2.247(2)	2.292(3)	1.912(1)	1.908(2)	1.946(3)
M–N4	-	2.052(2)	2.044(2)	1.797(1)	1.797(2)	1.799(3)
C11–N1–C2	120.7(1)	118.7(2)	120.9(3)	121.71(13)	118.4(2)	120.2(3)
C111–N10–C9	119.6(1)	122.2(2)	119.8(3)	119.06(13)	119.6(2)	122.6(3)
C11–N1–C2–C201	178.6(1)	-4.3(4)	-9.5(5)	-1.6(3)	1.9(3)	-3.8(5)
C111–N10–C9–C901	-177.1(1)	5.8(5)	6.4(5)	-2.3(2)	0.9(3)	-1.3(5)
C202–C201–C2–N1	-17.3(2)	-53.0(5)	-50.4(5)	-66.9(3)	-	-
C902–C901–C9–N10	-4.3(2)	-49.8(5)	63.4(5)	47.0(2)	-	-
C12–C11–N1–C2	99.6(2)	111.2(3)	106.8(4)	103.6(2)	90.0(3)	-79.1(4)
C112–C111–N10–C9	90.2(2)	112.1(3)	-98.3(4)	-107.5(2)	-100.6(3)	111.6(4)
N4–C3–C2–N1	-67.3(2)	-7.4(4)	-11.0(4)	-1.5(2)	-1.4(3)	-2.7(4)
N4–C8–C9–N10	-85.5(2)	-4.5(4)	8.7(5)	2.4(2)	-0.7(3)	2.9(4)
N1–M–N10	-	142.34(9)	145.62(10)	163.34(6)	162.95(8)	162.74(12)
N1–M–N4	-	74.64(9)	75.09(11)	81.67(6)	81.37(8)	81.52(13)
N10–M–N4	-	73.16(9)	74.63(10)	81.73(6)	81.58(8)	81.59(13)
M–Cl1	-	2.233(1)	2.231(1)	2.176(1)	2.179(1)	1.946(3) ^a
M–Cl2	-	2.332(1)	2.294(1)	-	-	-
N4–M–Cl2	-	91.09(7)	92.70(8)	-	-	-
N4–M–Cl1	-	150.69(8)	145.42(9)	173.43(5)	179.55(7)	171.24(13) ^a
Cl1–M–Cl2	-	118.19(4)	121.87(4)	-	-	-

^a Co–N(pyridine).**Figure 2.** Molecular structure of the iron complex **9**. Selected bond lengths (Å) and angles (deg): N1–C11 1.452(4), C2–C3 1.483(4), C3–N4 1.348(3), N4–C8 1.349(4), C8–C9 1.487(4), N10–C111 1.448(4); Fe–N1–C11 125.8(2), Fe–N1–C2 115.3(2), N1–C2–C3 115.6(2), C2–C3–N4 113.5(3), C3–N4–C8 120.2(3), Fe–N4–C3 119.4(2), Fe–N4–C8 119.6(2), N4–C8–C9 113.4(3), C8–C9–N10 114.7(3), Fe–N10–C9 113.6(2), Fe–N10–C111 122.7(2). For additional values see Table 1 and the text.

102.68(7)° (N1–Fe–Cl2), 91.09(7)° (N4–Fe–Cl2), 96.96(7)° (N10–Fe–Cl2), and especially in the characteristic Cl1–Fe–Cl2 angle of 118.19(4)°. The Fe–N(pyridyl) bond in complex **9** is markedly shorter than the Fe–N1/N10 (imino) linkages ($\Delta\delta \sim 0.2$ Å; see Table 1). The bulky 2,6-diisopropylphenyl substituents at the imino-nitrogen centers N1 and N10 are rotated close to normal to the basal plane of the complex, and also the phenyl substituents at the iminocarbon atoms are markedly rotated out of the plane of the Schiff-base functional groups, probably to avoid steric interaction with the bulky adjacent aryl substituents but also to avoid contact with the central pyridyl group. It is noteworthy that the rotation of the phenyl groups at C9 and at C2 are equal with regard to the resulting chirality element. Thus, complex **9** adopts a chiral conformational arrangement in the crystal (for the values of the corresponding dihedral angles, see Table 1).

**Figure 3.** A view of the molecular structure of the cobalt complex **10**. Selected bond lengths (Å) and angles (deg): N1–C11 1.436(5), C2–C3 1.492(5), C3–N4 1.337(4), N4–C8 1.335(4), C8–C9 1.489(5), N10–C111 1.432(4); Cl1–Co–N1 97.40(8), Cl1–Co–N10 98.30(7), Cl2–Co–N1 97.49(8), Cl2–Co–N10 99.81(8), Co–N1–C11 125.3(2), Co–N1–C2 113.5(2), N1–C2–C3 115.3(3), C2–C3–N4 114.6(3), C3–N4–C8 121.1(3), Co–N4–C3 117.4(2), Co–N4–C8 118.3(2), N4–C8–C9 114.9(3), C8–C9–N10 116.7(3), Co–N10–C9 111.9(2), Co–N10–C111 128.3(2).

The cobalt(I) chloride complexes **11**, **13**, and **15** all feature a distorted square-planar coordination of the central metal atom. In **11** the N1–Co–N10 angle amounts to 163.34(6)° (which is by ca. 20° larger than that found in **9** or **10**), and the corresponding N4–Co–Cl angle in **11** is even closer to linear at 173.43(5)°. The “intra-chelate angles” at Co are both close to 81° (see Table 1), whereas the remaining pair of ligand angles at cobalt amount to 98.89(4)° (N1–Co–Cl1) and 97.77(4)° (N10–Co–Cl1) (the sum of “inplane” bonding angles at cobalt is 360.06°). The central Co–N4 bond to the pyridine moiety is by $\Delta\delta$ 0.11 Å shorter than the lateral Co–N1/N2 distances. Again, the bulky 2,6-diisopropylphenyl moieties at the imino-nitrogens are rotated close to normal to the chelate ligand plane, and the phenyl substituents at the C=N carbon atoms are also rotated markedly (see Table 1 for the respective dihedral angles). In **11** both these phenyl groups were found to be rotated in

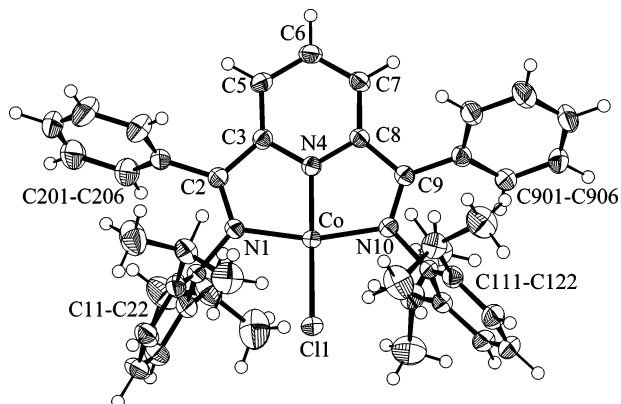


Figure 4. Molecular structure of the [bis(*N*-aryliminobenzyl)pyridine]Co(DCl) complex **11**. Selected bond lengths (Å) and angles (deg): N1–C11 1.445(2), C2–C3 1.446(2), C3–N4 1.373(2), N4–C8 1.370(2), C8–C9 1.446(2), N10–C111 1.439(2); Co–N1–C11 122.1(1), Co–N1–C2 115.9(1), N1–C2–C3 112.9(1), C2–C3–N4 109.9(1), C3–N4–C8 120.7(1), Co–N4–C3 119.6(1), Co–N4–C8 119.7(1), N4–C8–C9 110.0(1), C8–C9–N10 112.6(1), Co–N10–C9 115.8(1), Co–N10–C111 125.0(1). For additional values see the text and Table 1.

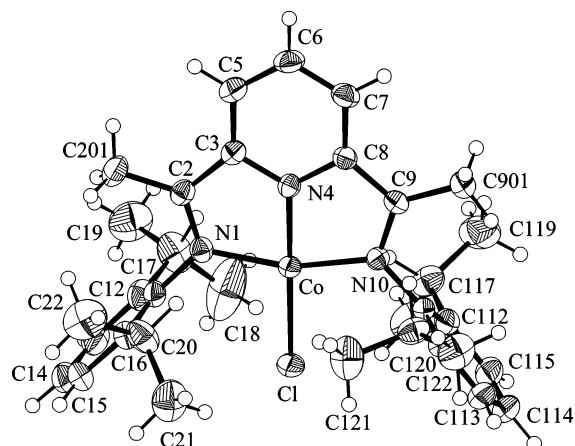


Figure 5. A view of the molecular structure of complex **13**. Selected bond lengths (Å) and angles (deg): N1–C11 1.442(3), C2–C3 1.435(3), C3–N4 1.369(3), N4–C8 1.368(3), C8–C9 1.434(3), N10–C111 1.443(3); C11–Co–N1 98.92(6), C11–Co–N10 98.12(6), Co–N1–C11 125.7(2), Co–N1–C2 115.9(2), N1–C2–C3 113.2(2), C2–C3–N4 109.6(2), C3–N4–C8 120.7(2), Co–N4–C3 119.9(2), Co–N4–C8 119.4(2), N4–C8–C9 110.4(2), C8–C9–N10 112.6(2), Co–N10–C9 116.0(2), Co–N10–C111 124.5(2). For additional values, see Table 1.

opposite directions. In the crystal complex **11** thus adopts a close to achiral “meso-like” conformation (see Figure 4), similar to **10** (see Figure 3).

The closely related complex **13** (see Scheme 3) had previously been prepared by Gal et al.,⁷ but to the best of our knowledge, it had not been characterized by X-ray diffraction. In the crystal it features a distorted square-planar complex geometry with a rather short Co–N4 (1.797(2) Å) bond trans to Co–Cl (2.179(1) Å). As already seen in **11** the C=N bond lengths in **13** [N1–C2 1.322(3) Å, C9–N10 1.326(3) Å] are markedly longer than those in the (lig)CoCl₂ complex (**10**) or its (lig)-FeCl₂ analogue (**9**) (see above; see Figure 5).

In the [bis(*N*-aryliminoethyl- κ -N,N')pyridine- κ N]Co(pyridine)⁺·[B(C₆F₅)₄][−] salt **15**,¹⁶ cations and anions are well separated. The cobalt(I) center in the cationic part features the typical

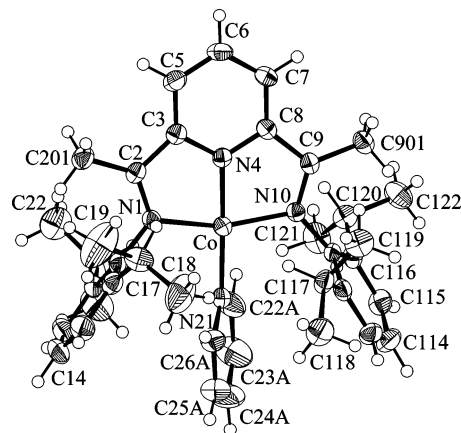


Figure 6. A projection of the molecular structure of the cation part of complex **15**. Selected bond lengths (Å) and angles (deg): N1–C11 1.440(5), C2–C3 1.446(5), C3–N4 1.372(4), N4–C8 1.365(4), C8–C9 1.463(5), N10–C111 1.447(4); N21A–Co–N1 99.4(1), N21A–Co–N10 97.9(1), Co–N1–C11 123.4(2), Co–N1–C2 116.1(2), N1–C2–C3 113.0(3), C2–C3–N4 109.9(3), C3–N4–C8 120.6(3), Co–N4–C3 119.3(2), Co–N4–C8 120.1(2), N4–C8–C9 109.9(3), C8–C9–N10 113.3(3), Co–N10–C9 115.1(2), Co–N10–C111 122.3(2). Further values are listed in Table 1.

square-planar coordination geometry with the three nitrogen atoms of the chelate ligand showing the typical sequence of bond lengths to cobalt (Figure 6). In the cation **15** the C=N bonds are slightly shorter than those in the related neutral Co(DCl) complex **13** (for details see Table 1). A single pyridine ligand is coordinated at cobalt trans to the chelate pyridine moiety (Co–N4 1.799(3) Å vs Co–N21A 1.946(3) Å). The plane of the single pyridine ligand is rotated from the central (N₄Co) plane by 64.2°. Again, the bulky 2,6-diisopropylphenyl groups at the imino nitrogen centers N1 and N10 are oriented with their aryl planes close to orthogonal to the major coordination plane.

The structure of the free ligand **22** [(lig^{OMe})] shows a conformation that features one C=N nitrogen (N1) oriented to the inside of the pincer chelate and the other (N3) oriented away from the pyridine nitrogen (Figure 7).

This structural motive is retained in the complexes **23** (FeCl₂) and **24** (CoCl₂). In **23** the ligand is strongly coordinated to iron through both nitrogen atoms and weakly to the oxygen atom of the remaining –C(=NAr)–OMe group (Fe–O1 2.5361(17) Å; see Figure 8 and Table 2). This deviates from the structure of the related complex **23a** (with Ar = mesityl) reported by Gibson et al.¹⁵ which features nitrogen coordination exclusively. In **23** the O1–C20 (1.450(3) Å) and O2–C21 (1.457(3) Å) bond lengths are slightly longer than typical carbon–oxygen single bonds, whereas the O1–C7 (1.353(3) Å) and O2–C13 (1.324(3) Å) bond lengths are shorter. The N1–C7 bond length (1.264(3) Å) exhibits a typical value for carbon–nitrogen double bonds, while the N3–C13 (1.285(3) Å) bond length is slightly elongated due to the nitrogen atom coordinating to iron. The geometry at the metal center can best be described as distorted trigonal bipyramidal. The equatorial plane is formed by the pyridine nitrogen atom and the two chloride ligands. The axial positions are occupied by the nitrogen atom N3 and the oxygen atom O1. The sum of the bond angles within the equatorial plane is 354.05° (N2–Fe–C11 101.55(6)°, N2–Fe–C12 131.13(6)°, C11–Fe–C12 121.37(3)°). The axial O1–Fe–N3 angle was found at 140.06(7)°.

(16) Kehr, G.; Roesmann, R.; Fröhlich, R.; Holst, C.; Erker, G. *Eur. J. Inorg. Chem.* **2001**, 535–538.

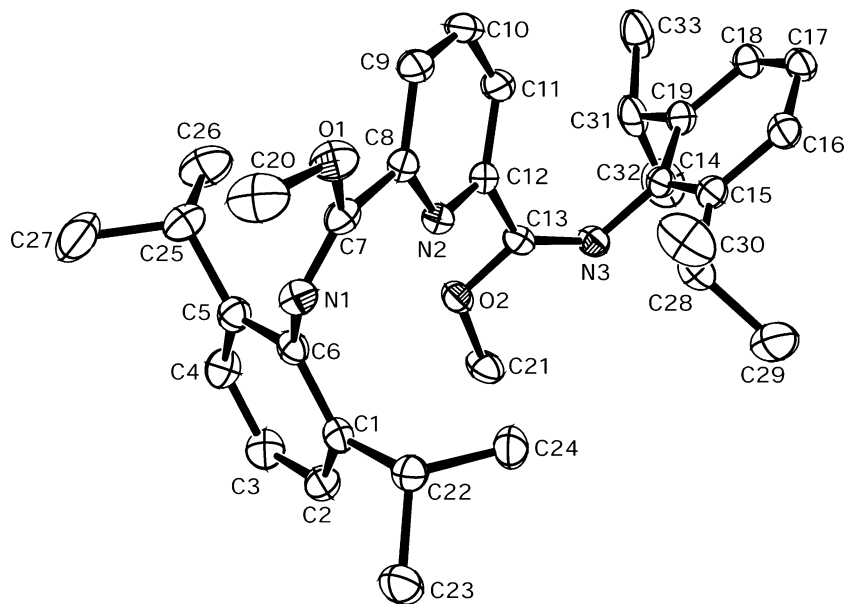


Figure 7. View of the molecular structure of the free ligand **22**.

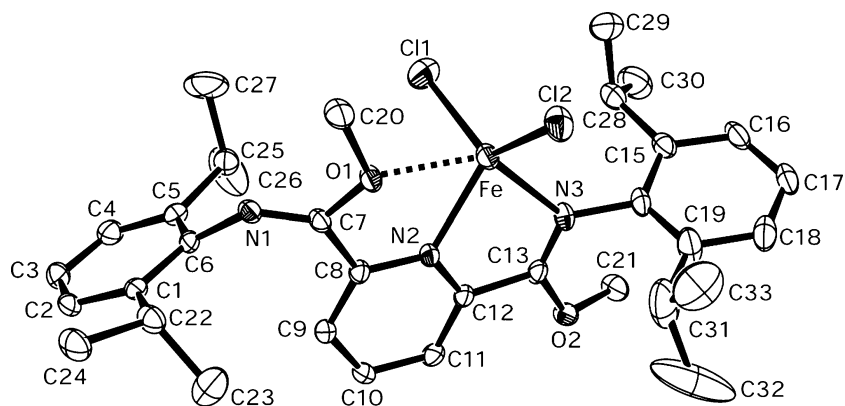


Figure 8. A view of the molecular structure of complex **23**.

The cobalt complex **24** (Figure 9) again exhibits a distorted trigonal bipyramidal geometry, featuring $\text{O}\wedge\text{N}\wedge\text{N}$ -coordination with a weak $\text{Co}-\text{O}1$ interaction (2.460(4) Å) with equatorial angles $\text{N}2-\text{Co}-\text{C}11$ 101.57(14)°, $\text{N}2-\text{Co}-\text{C}12$ 135.32(15)°, $\text{C}11-\text{Co}-\text{C}12$ 116.73(8)° ($\Sigma = 353.62^\circ$) and an axial $\text{O}1-\text{Co}-\text{N}3$ angle of 143.44(17)°.

Single crystals for the $\text{N}\wedge\text{N}\wedge\text{N}$ -coordinated (lig^{OMe}) CoCH_3 isomer **26** were grown from a toluene solution by pentane diffusion at room temperature (Figure 10). Similar as in **11**, **13**, and **15** (see above) the metal center is coordinated in a distorted square planar fashion. The metal coordination plane is spanned from $\text{N}(3)$ through the pyridine ring to $\text{N}(1)$ and $\text{C}(34)$ with the 2,6-diisopropylphenyl rings perpendicular to the plane. The $\text{Co}-\text{C}(34)$ bond length is 1.958(2) Å. Comparison between the $\text{Co}(\text{II})$ chloride species **24** and the $\text{Co}(\text{I})$ methyl species **26** shows a marked difference in the $\text{Co}-\text{N}$ bond lengths. A shortening of 0.20 to 0.23 Å was observed with reduction of cobalt (**24**: $\text{Co}-\text{N}(2) = 2.066(5)$ Å, $\text{Co}-\text{N}(3) = 2.103(5)$ Å; **26**: $\text{Co}-\text{N}(2) = 1.8359(14)$ Å, $\text{Co}-\text{N}(1) = 1.9066(14)$ Å, $\text{Co}-\text{N}(3) = 1.9057(14)$ Å).

The cationic $\text{Co}(\text{I})$ complex **27** features a different structure than the chemically related $[(\text{lig}^{\text{Me}})\text{Co}^+-\text{pyridine}]$ complex **15** (see above). In **27** the cobalt center is coordinated by the pyridine nitrogen, one imine nitrogen, and one η^6 -aryl ring (see

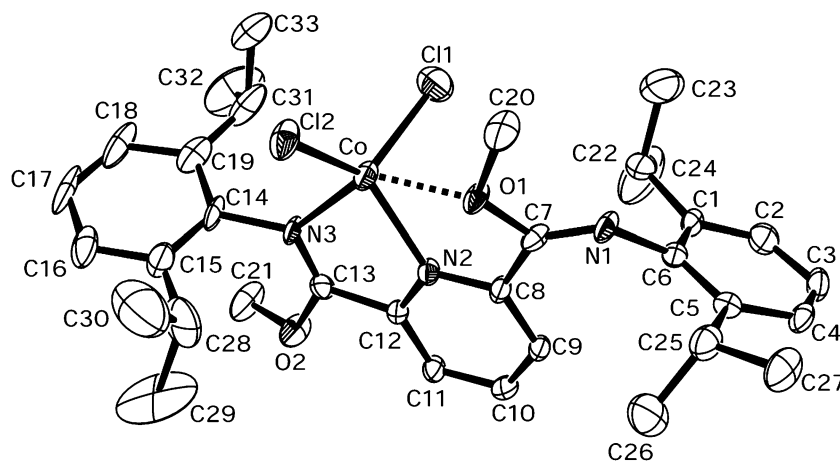
Figure 11). The metal coordination plane is spanned from the coordinating iminoester nitrogen through the pyridine ring. The 2,6-diisopropylphenyl rings are perpendicular to the plane. The $\text{Co}-\text{N}$ bonds are comparable in lengths to those of the neutral precursor **26** ($\text{Co}-\text{N}1 = 1.8904(19)$ Å, $\text{Co}-\text{N}2 = 1.8645(19)$ Å). The bond distances for the $\text{Co}-\text{C}$ bonds of the η^6 -coordinated aryl ring were found between 2.03 and 2.15 Å. Attempts to stabilize this $\text{Co}(\text{I})$ complex with pyridine were not successful.

Ethene Polymerization: Preliminary Results. The (lig)- CoCH_3 complexes **16** and **17** themselves were found to be inactive toward ethene in the absence of a suitable activator. Treatment of the $[\text{bis}(\text{iminoethyl})\text{pyridine}]\text{CoCH}_3$ complex **17** with $\text{B}(\text{C}_6\text{F}_5)_3$ gave an active ethene polymerization catalyst. In a typical experiment 50 mg of **17** were reacted with 1 molar equiv of $\text{B}(\text{C}_6\text{F}_5)_3$. The mixture was allowed to react with ethene (30 min, toluene, room temperature, 2 bar ethene pressure) to yield ca. 1.4 g of linear polyethylene (average yield from two experiments), which corresponds to an averaged polymerization activity of $a = 16 \text{ g(PE) mmol(catalyst)}^{-1} \text{ h}^{-1} \text{ bar}^{-1}$. Likewise, polyethylene was formed at the **16**/ $\text{B}(\text{C}_6\text{F}_5)_3$ catalyst system. A similar (rather low) activity was found in this case ($a = 15 \text{ g(PE) mmol(catalyst)}^{-1} \text{ h}^{-1} \text{ bar}^{-1}$).

Table 2. Selected Structural Data of the Chelate Ligand **22** and the Complexes **23**, **24**, **26**, and **27**

compound ML _n	22 -	23 FeCl ₂	24 CoCl ₂	26 CoMe	27 Co ⁺
C7–N1	1.2609(16)	1.264(3)	1.249(7)	1.318(2)	1.307(3)
C13–N3	1.2647(15)	1.285(3)	1.278(7)	1.318(2)	1.268(3)
C7–O1	1.3543(14)	1.353(3)	1.351(7)	1.356(2)	1.394(3)
C20–O1	1.4387(18)	1.450(3)	1.458(7)	1.427(3) ^a	1.315(6) ^a
C13–O2	1.3394(14)	1.324(3)	1.334(7)	1.350(2)	1.343(3)
C21–O2	1.4420(15)	1.457(3)	1.462(7)	1.422(3) ^a	1.440(3)
M–N1	-	-	-	1.9057(14)	1.8904(19)
M–N2	-	2.147(2)	2.066(5)	1.8359(14)	1.8645(19)
M–N3	-	2.158(2)	2.103(5)	1.9066(14)	-
M–O1	-	2.5361(17)	2.460(4)	-	-
M–Cl	-	2.2517(8)	2.237(2)	-	-
M–Cl	-	2.2672(8)	2.2384(19)	-	-
M–C	-	-	-	1.9580(19)	-
C6–N1–C7	125.16(10)	129.8(2)	129.0(5)	118.56(14)	121.1(2)
C13–N3–C14	121.50(10)	120.7(2)	120.7(5)	119.09(14)	121.5(2)
N2–M–N3	-	76.95(8)	79.16(19)	81.33(6)	-
N2–M–O1	-	66.55(7)	67.71(17)	-	-
N3–M–O1	-	140.06(7)	143.44(17)	-	-
N1–M–N3	-	-	-	162.90(6)	-
N2–M–Cl1	-	101.55(6)	101.57(14)	-	-
N2–M–Cl2	-	131.13(6)	135.32(15)	-	-
N1–M–C34	-	-	-	98.16(8)	-
N2–M–C-34	-	-	-	174.55(10)	-
N3–M–C34	-	-	-	98.81(8)	-
C11–M–Cl2	-	121.37(3)	116.73(8)	-	-
C1–C6–N1–C7	113.51(14)	-73.5(3)	71.7(9)	88.7(2)	-99.3(3)
C15–C14–N3–C13	76.09(16)	110.8(3)	74.0(8)	100.97(18)	-98.9(3)
N2–C8–C7–N1	-22.6(2)	162.3(2)	-162.9(7)	3.4(2)	-
N2–C12–C13–N3	-132.80(14)	0.9(3)	2.4(9)	-4.3(2)	10.5(4)

^a C20 is C32 and C21 is C33 in this compound.

**Figure 9.** A view of the molecular structure of complex **24**.

Treatment of the [bis(iminoethyl)pyridine]CoCH₃ complex **17** with 1 molar equivalent of Li[B(C₆F₅)₄] in toluene followed by exposure of the solution to ethene again resulted in the formation of polyethylene with a similar activity. Starting from 50 mg (0.090 mmol) of **17** and 62 mg (0.090 mmol) of lithium tetrakis(pentafluorophenyl) borate resulted in the formation of 1.70 and 2.22 g, respectively, of polyethylene in two independent experiments (30 min, room temperature, toluene, 2 bar ethene pressure) which corresponds to an average catalyst activity of $a = 22 \text{ g(PE) mmol(catalyst)}^{-1} \text{ h}^{-1} \text{ bar}^{-1}$. A set of similar experiments was carried out starting from the [bis(iminobenzyl)pyridine]CoCH₃ complex **16**. Treatment with an equimolar quantity of Li[B(C₆F₅)₄] again gave an active catalyst; starting from 50 mg of **16** we obtained ca. 2.4 g of PE under the typical reaction conditions (see above), which corresponds to an

averaged catalyst activity of $a = 33 \text{ g(PE) mmol(catalyst)}^{-1} \text{ h}^{-1} \text{ bar}^{-1}$. In CH₂Cl₂ a similar catalyst activity was obtained.

Complex [(lig^{Ph})CoCH₃] (**16**) could even be activated by treatment with a Brønsted acid, provided that an inert anion was employed. The reaction of **16** with the H⁺ acidic 2*H*-pyrrol-B(C₆F₅)₃ adduct **28**¹⁶ also gave an active catalyst for polyethylene formation (see Scheme 5 and Table 3). In this case the catalytically active metal cation complex is accompanied by the poorly nucleophilic [(*N*-pyrrol)-B(C₆F₅)₃]⁻ counteranion.

Ethene polymerization with compound **23** activated by MAO resulted in low activity (3 g(PE) mmol(**23**)⁻¹ h⁻¹ bar⁻¹). Activation with MAO/B(C₆F₅)₃ did not result in a change of activity, and activation with MAO/BF₃ gave only a slightly more active catalyst (8 g(PE) mmol(**23**)⁻¹ h⁻¹ bar⁻¹).

Compounds **25/26** themselves did not show any ethene

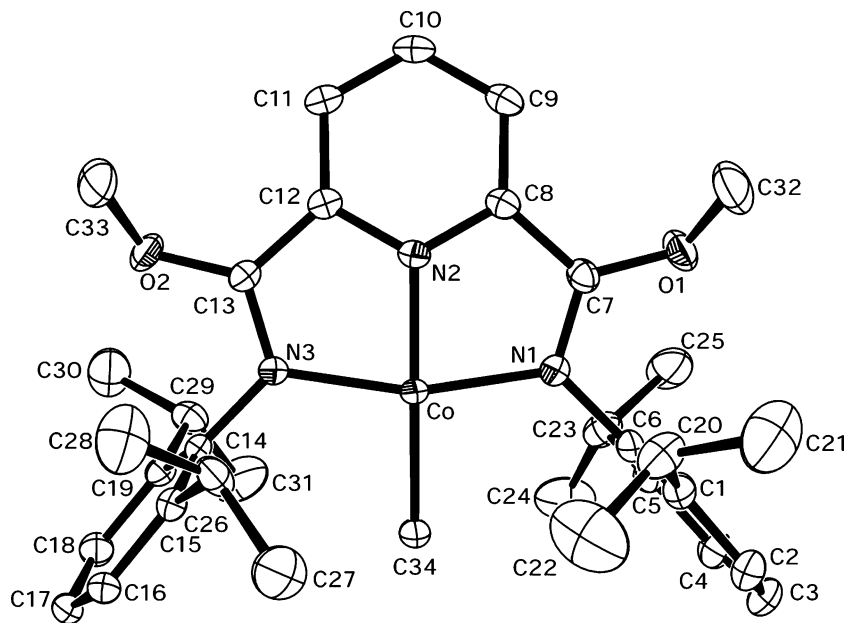


Figure 10. A view of the molecular structure of the Co(I) complex 26.

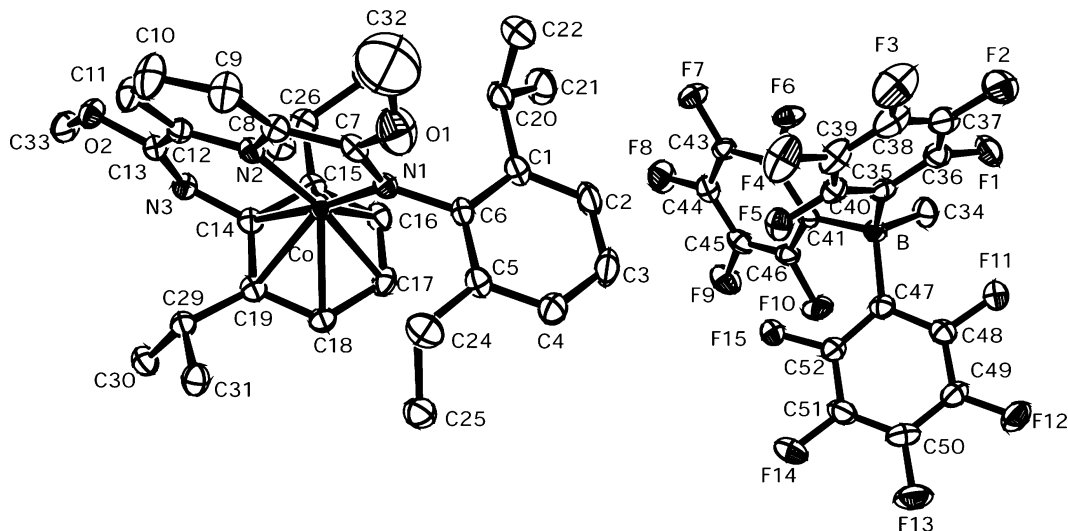
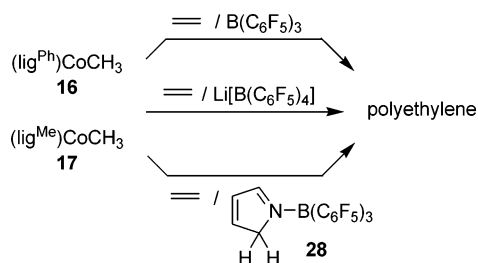


Figure 11. A view of the molecular structure of complex 27.

Scheme 5



polymerization activity without cocatalyst under the applied reaction conditions. Activation with $\text{B}(\text{C}_6\text{F}_5)_3$ or generation of compound 27 *in situ* in this case did not result in an active species for ethene polymerization, and no color change was observed after the introduction of ethene. Activation of the isomeric mixture 25/26 with $\text{Li}[\text{B}(\text{C}_6\text{F}_5)_4]$ resulted in polyethylene formation (Scheme 6) with an average activity of $a = 36 \text{ g mmol}(\mathbf{25}/\mathbf{26})^{-1} \text{ h}^{-1} \text{ bar}^{-1}$. The reaction mixture stayed purple upon the addition of $\text{Li}[\text{B}(\text{C}_6\text{F}_5)_4]$ and turned grayish after the

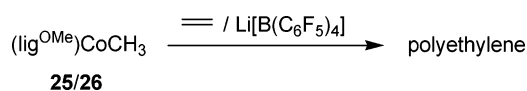
Table 3. Ethene Polymerization Activities of the Catalysts Derived from the $(\text{lig})^x\text{CoL}_n$ Complexes and Different Activators^a

no. (ML _n /X)	no activator	Li ⁺	H ⁺	$\text{B}(\text{C}_6\text{F}_5)_3$	MAO	MAO/BF ₃
10 (CoCl ₂ /Ph)		n.a.				
12 (CoCl ₂ /Me)		n.a.				
24 (CoCl ₂ /OMe)		n.a.				12
11 (CoCl/Ph)		n.a. ^c		n.a.		
13 (CoCl/Me)		– ^c		n.a.		
16 (CoMe/Ph)	n.a.	33	5 ^b	15 ^b		
17 (CoMe/Me)	n.a.	22 ^b		16 ^b		
25/26 (CoMe/OMe)	n.a.	36		n.a.	7	37

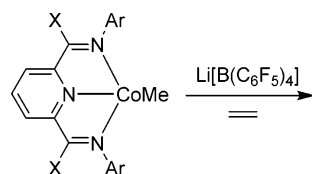
^a n.a.: no activity; ^a = g(PE) mmol(cat.)⁻¹ h⁻¹ bar⁻¹. ^b Average value from several polymerization reactions. ^c See ref. 19.

introduction of ethene. In comparison, compound 25/26 resulted in a ca. 3-fold more active species upon activation with $\text{Li}[\text{B}(\text{C}_6\text{F}_5)_4]$ than compound 24 activated with MAO/BF₃ (see Table 3). While the catalyst derived from the Co(II) dichloride complex 24 gave rise to low molecular weight polymer ($M_n = 617 \text{ g mol}^{-1}$) with narrow molecular weight distribution ($M_w/M_n = 1.3$), the $(\text{lig}^{\text{OMe}})\text{Co}(\text{I})$ methyl derived 25/26/ $\text{Li}[\text{B}(\text{C}_6\text{F}_5)_4]$

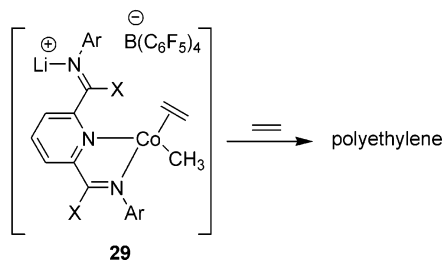
Scheme 6



Scheme 7



16 (X = Ph)
17 (X = Me)
26 (X = OMe)



catalyst provided slightly higher molecular weight polymers (>2000), which were mostly bimodal with broader molecular weight distributions ($M_w/M_n = 1.5$ to 7.6).

Conclusions

The **16/17**/ $\text{B}(\text{C}_6\text{F}_5)_3$ system could potentially correspond to the members of the small family of catalyst systems shown in Scheme 1. The observation that a catalyst system, albeit of rather low ethene polymerization activity, was formed upon treatment of the precursors **16,17** or **25/26** with Li^+ seems not to be in accord with the proposed olefin polymerization pathways at such catalyst systems but indicates the occurrence of a different activation mode. A clarification of the actual pathway followed in these $(\text{lig})\text{CoCH}_3/\text{Li}[\text{B}(\text{C}_6\text{F}_5)_4]$ /ethene systems must await further experimental evidence. Possibly the Li^+ cation might interact with one “arm” of the chelate donor ligand, which would create an open coordination site at a reactive overall cationic reactive intermediate (e.g., **29**; see Scheme 7). In the system **27** (see Scheme 4) we had already observed that an imino-nitrogen coordination can easily be “lost” upon metal cation formation if some suitable ligand is available for additional stabilization. In a possible Ziegler–Natta reactive intermediate (**29**, see Scheme 7) this could possibly be an incoming ethene monomer. The observation that **16** can be activated by protonation using the special Brønsted acid **28** could potentially be explained by a similar mechanism where an imine coordination from the former tridentate ligand system would be removed by internal iminium ion formation. A variety of mechanistic alternatives could be discussed at this stage of the investigation but must await further detailed experimental studies.

In view of these surprising results we cannot rule out that the very low activity polyethylene formation that we had recently observed at the $(\text{lig})\text{CoCl}(\mathbf{11},\mathbf{13})/\text{Li}[\text{B}(\text{C}_6\text{F}_5)_4]$ systems¹⁸ was not intrinsic but may have been caused by some as yet unidentified cobalt alkyl contaminant.¹⁹ With such low polymerization activities there is always the possibility that the observed reaction is caused by a minor high activity contamination. However, our observation that the $(\text{lig})\text{CoCH}_3/\text{Li}[\text{B}(\text{C}_6\text{F}_5)_4]$ systems produce

polyethylene potentially indicates that other Lewis acid or Brønsted acid activators might activate organometallic precursors by some ligand specific reaction pathways (potentially being operative out of an equilibrium with other cationic species) other than previously assumed. It needs to be explored whether such pathways might also be of importance in the more active homogeneous Ziegler–Natta systems of this general type such as, e.g., the $(\text{lig})\text{FeCl}_2$ derived polymerization catalysts or in some of the early metal systems depicted in Scheme 1.

Experimental Section

General Procedures. Reactions with organometallic substrates or reagents were carried out in an inert atmosphere (Ar) using Schlenk-type glassware or in a glovebox. Solvents were dried and distilled under argon prior to use. NMR spectra were recorded with a Varian UNITYplus 600 (^1H : 599.9 MHz, ^{13}C : 150.8 MHz) spectrometer or a Varian UNITY INOVA 400 MHz (^1H : 399.9 MHz, ^{13}C : 100.6 MHz). An unsystematical atom numbering scheme analogous to that in Table 1 and Figures 1 to 6 is used. Most assignments were based on additional 2D NMR spectra.²⁰ The following instruments were used for additional physical characterization: IR spectroscopy, Nicolet 5DXC FT-IR spectrometer; melting points, DSC 2010 TA instruments); elemental analysis, Elementar Vario ELIII, Leeman Labs Inc. CE440 Elemental Analyzer or a Control Equipment Corporation 440 Elemental Analyzer. 2,6-Dibenzoylpyridine (**7**)¹² and the $[\text{bis}(N\text{-aryliminoethyl-}\kappa N,N')\text{-pyridine-}\kappa N]\text{CoCl}_2$ complex (**12**)^{9a} were prepared according to literature procedures. Complex **13** had been described previously⁷ but was prepared here by a different reducing method. $\text{Li}[\text{B}(\text{C}_6\text{F}_5)_4]$ (**18**) was prepared by treatment of freshly prepared $\text{Li}(\text{C}_6\text{F}_5)$ (warning: this compound is explosive and must be handled with care at low temperature) with 0.25 equiv of BCl_3 at -78°C . The obtained white solid was collected and extracted with toluene, followed by two successive fractional recrystallizations of the crude product from toluene. The $(\text{lig})\text{CoCH}_3$ complexes were usually freshly prepared prior to their use in the polymerization experiments.

Data sets were collected with Enraf-Nonius CAD4 and Nonius KappaCCD diffractometers, the later one equipped with a rotating anode generator Nonius FR591. Programs used: data collection EXPRESS (Nonius B.V., 1994) and COLLECT (Nonius B.V., 1998), data reduction MolEN (K. Fair, Enraf-Nonius B.V., 1990) and Denzo-SMN (Z. Otwinowski, W. Minor, *Methods in Enzymology*, **1997**, 276, 307–326), absorption correction for CCD data SORTAV (R. H. Blessing, *Acta Cryst.* **1995**, A51, 33–37; R. H. Blessing, *J. Appl. Cryst.* **1997**, 30, 421–426), structure solution SHELXS-97 (G. M. Sheldrick, *Acta Cryst.* **1990**, A46, 467–473), structure refinement SHELXL-97 (G. M. Sheldrick, Universität Göttingen, 1997), graphics Diamond (K. Brandenburg, Universität Bonn, 1997). For the structures of **22–24**, **26**, and **27**, the single crystal was mounted on a glass fiber and transferred to a Bruker CCD platform diffractometer. The SMART program package (SMART Software Users Guide, version 5.1; Bruker Analytical X-ray Systems, Inc.; Madison, WI, 1999) was used to determine the unit-cell parameters and for data collection (25 s/frame scan time for

(17) Erker, G.; Frömberg, W.; Krüger, C.; Raabe, E. *J. Am. Chem. Soc.* **1988**, 110, 2400–2405.

(18) Steffen, W.; Blömker, T.; Kleigrew, N.; Kehr, G.; Fröhlich, R.; Erker, G. *Chem. Commun.* **2004**, 1188–1189.

(19) We have carried out a number of additional series of control experiments. In a series of four experiments using the $[\text{bis}(2,6\text{-diisopropylphenylimino-}\kappa N,N'\text{-ethyl)pyridine-}\kappa N]\text{CoCl}$ system **13**, freshly prepared by treatment of **12** with butadiene-magnesium, an average of 177 mg of PE was isolated (under typical conditions [50 mg (0.087 mmol) of **13**, 59.6 mg (0.087 mmol) of $\text{Li}[\text{B}(\text{C}_6\text{F}_5)_4]$, toluene, rt, 2 bar ethene pressure]). An additional experiment carried out with independently prepared starting materials gave only 32 mg of PE under the same conditions. A $[\text{bis}(2,6\text{-diisopropylphenylimino-}\kappa N,N'\text{-benzyl)pyridine-}\kappa N]\text{CoCl}$ (**11**) sample, synthesized from **10** by the butadiene-magnesium method, gave no PE under equivalent reaction conditions after $\text{Li}[\text{B}(\text{C}_6\text{F}_5)_4]$ treatment.

(20) Braun, S.; Kalinowski, H. O.; Berger, S. *150 and More Basic NMR Experiments*; VCH: Weinheim, 1998 and references therein.

a sphere of diffraction data). The raw frame data were processed using SAINT (SAINT Software Users Guide, version 6.0; Bruker Analytical X-ray Systems, Inc.: Madison, WI, 1999) and SADABS (Sheldrick, G. M. SADABS, version 2.05, Bruker Analytical X-ray Systems, Inc.: Madison, WI, 2001) to yield the reflection data file. Subsequent calculations were carried out using the SHELXTL (Sheldrick, G. M. SHELXTL version 6.12, Bruker Analytical X-ray Systems, Inc.: Madison, WI, 2001) program. The structure was solved by direct methods and refined on F^2 by full-matrix least-squares techniques. The analytical scattering factors (International Tables for X-ray Crystallography; Kluwer Academic Publishers: Dordrecht, 1992; Vol. C) for neutral atoms were used throughout the analysis.

Condensation of 2,6-Dibenzoylpyridine with 2,6-Diisopropylaniline. Synthesis of the Ligand System 8: 2,6-Dibenzoylpyridine (5.00 g, 17.4 mmol), 2,6-diisopropylaniline (6.79 g, 38.3 mmol), and a catalytic quantity of *p*-toluenesulfonic acid (221 mg, 1.15 mmol) were dissolved in 50 mL of toluene. The mixture was refluxed for 12 h using a Dean–Stark trap to remove the water. Solvent was removed in vacuo, and the residue was purified by column chromatography (silicagel, pentane/triethylamine/chloroform: 50/3/3). Two yellow fractions were obtained that both contained the product. The volume of the first fraction was reduced in vacuo to ca. 10 mL. Single crystals for the X-ray crystal structure analysis were formed overnight at ambient temperature. The product from both fractions was used for the subsequent reactions; yield of **8**: 5.71 g, 54%, mp 142 °C; IR (KBr): $\tilde{\nu}$ = 2960, 1653, 1446, 1315, 937 cm^{-1} . MS (70 eV, EI): m/z = 605 (100%, M^+). MS (ESI+): m/z = 606.4 ($[\text{M} + \text{H}]^+$), 628.5 ($[\text{M} + \text{Na}]^+$). Anal. Calcd for $\text{C}_{43}\text{H}_{47}\text{N}_3$ (605.9): C, 85.25; H, 7.82; N, 6.94. Found: C, 85.09; H, 7.73; N, 6.94%. ^1H NMR (CDCl_3 , 298 K): δ 8.54, 8.12, 8.04, 7.94, 7.66, 7.54–7.31, 7.23–6.99 (each very broad, 19H), 3.05, 2.95, 2.87 (each very broad, 4H), 1.18, 1.02, 0.96 (each very broad, 24H) (The system is dynamic).

X-ray crystal structure analysis of **8**: formula $\text{C}_{43}\text{H}_{47}\text{N}_3$, M = 605.84, light yellow crystal $0.35 \times 0.25 \times 0.25 \text{ mm}^3$, a = 19.736(2) Å, b = 11.967(1) Å, c = 16.077(2) Å, β = 106.03(1)°, V = 3649.4(7) Å³, ρ_{calcd} = 1.103 g cm^{-3} , μ = 4.84 cm^{-1} , empirical absorption correction via ψ -scan data ($0.849 \leq T \leq 0.889$), Z = 4, monoclinic, space group $P2_1/c$ (No. 14), λ = 1.54178 Å, T = 223 K, $\omega/2\theta$ scans, 7632 reflections collected ($-h$, $+k$, $\pm l$), $[(\sin \theta)/\lambda]$ = 0.62 Å⁻¹, 7413 independent (R_{int} = 0.027) and 5524 observed reflections [$I \geq 2\sigma(I)$], 424 refined parameters, R = 0.049, wR^2 = 0.153, max residual electron density 0.27 (–0.21) e Å^{-3} , hydrogens calculated and refined as riding atoms.

Reaction of 8 with FeCl_2 . Synthesis of Complex 9: A flame-dried Schlenk flask was charged under argon with iron(II) dichloride (0.24 g, 1.88 mmol) and *n*-butanol (50 mL). To another Schlenk flask, the Schiff base **8** (1.14 g, 1.88 mmol) and *n*-butanol (50 mL) were added under inert conditions. Both Schlenk flasks were heated to 80 °C for 1 h, and then the green FeCl_2/n -BuOH solution was transferred to the reaction vessel under argon, which contained the yellow suspension of the chelate ligand. The reaction mixture was heated further for 30 min at 80 °C, and then it was stirred for 12 h at room temperature. Subsequently the solvent was removed in vacuo, and the precipitated crude product **9** was washed with pentane until the solvent is colorless. The solid was collected by filtration and dried in vacuo to give **9** as a blue amorphous solid (1.12 g, 1.53 mmol, 81%). Slow crystallization from a saturated acetone solution gave single crystals of **9** for the X-ray crystal structure analysis. IR (KBr): $\tilde{\nu}$ = 3055, 2951, 2923, 2863, 1564, 1464, 1441, 1384, 1321, 1269, 1154, 1102, 1054, 1038, 807, 779, 699 cm^{-1} . Anal. Calcd for $\text{C}_{43}\text{H}_{47}\text{N}_3\text{Cl}_2\text{Fe}$ (732.6): C, 70.50; H, 6.47; N, 5.74. Found: C, 69.51; H, 6.88; N, 5.04%.

X-ray crystal structure analysis of **9**: formula $\text{C}_{43}\text{H}_{47}\text{N}_3\text{Cl}_2\text{Fe} \cdot 0.5\text{C}_7\text{H}_8$, M = 778.65, yellow crystal $0.25 \times 0.08 \times 0.05 \text{ mm}^3$, a = 13.521(1) Å, b = 16.290(1) Å, c = 19.298(1) Å, β = 98.26(1)°, V = 4206.4(5) Å³, ρ_{calcd} = 1.230 g cm^{-3} , μ = 5.20 cm^{-1} , empirical absorption correction ($0.881 \leq T \leq 0.975$), Z = 4, monoclinic, space

group $P2_1/c$ (No. 14), λ = 0.710 73 Å, T = 198 K, ω and φ scans, 14 059 reflections collected ($\pm h$, $\pm k$, $\pm l$), $[(\sin \theta)/\lambda]$ = 0.59 Å⁻¹, 7403 independent (R_{int} = 0.058) and 5005 observed reflections [$I \geq 2\sigma(I)$], 484 refined parameters, R = 0.051, wR^2 = 0.102, max residual electron density 0.63 (–0.56) e Å^{-3} , disordered toluene solvent molecule refined with split positions, fixed occupancies (twice 0.25), and geometrical constraints, hydrogens calculated and refined as riding atoms.

Reaction of 8 with CoCl_2 . Preparation of Complex 10: A flame-dried 200 mL Schlenk flask was charged under argon with the Schiff base **8** (3.12 g, 6.45 mmol) and dry *n*-butanol (50 mL). To another flame-dried 50 mL Schlenk flask CoCl_2 (0.84 g, 6.45 mmol) and dry *n*-butanol (20 mL) were added under inert conditions. Both Schlenk flasks were heated to 80 °C for 15 min, and then the blue CoCl_2/n -BuOH solution was transferred to the reaction vessel under argon, which contained the yellow suspension of the chelate ligand. The reaction mixture was cooled to room temperature during 15 min and then stirred for 12 h. The volume of the mixture was reduced to ca. 10 mL, and dry pentane was added. The precipitated product (**10**) was collected by filtration and dried in vacuo to give **10** as a yellow-brown amorphous solid (yield 3.88 g, 98%) that was used in the subsequent reduction reaction without further characterization. Single crystals were obtained from acetone.

X-ray crystal structure analysis of **10**: formula $\text{C}_{43}\text{H}_{47}\text{C}_{12}\text{N}_3\text{Co} \cdot \text{C}_3\text{H}_6\text{O}$, M = 793.74, yellow crystal $0.50 \times 0.20 \times 0.05 \text{ mm}^3$, a = 9.439(1) Å, b = 25.767(1) Å, c = 9.547(1) Å, β = 113.02(1)°, V = 2137.1(3) Å³, ρ_{calcd} = 1.234 g cm^{-3} , μ = 5.63 cm^{-1} , empirical absorption correction ($0.766 \leq T \leq 0.972$), Z = 2, monoclinic, space group $P2_1$ (No. 4), λ = 0.710 73 Å, T = 198 K, ω and φ scans, 15 129 reflections collected ($\pm h$, $\pm k$, $\pm l$), $[(\sin \theta)/\lambda]$ = 0.68 Å⁻¹, 8937 independent (R_{int} = 0.034) and 7378 observed reflections [$I \geq 2\sigma(I)$], 486 refined parameters, R = 0.051, wR^2 = 0.122, max residual electron density 1.07 (–0.46) e Å^{-3} , Flack parameter 0.000(15), hydrogens calculated and refined as riding atoms.

Reduction of 10 by Treatment with Methylolithium. Synthesis of Complex 11: The [bis(imino)pyridine] CoCl_2 complex **10** (0.70 g, 0.95 mmol) was suspended in 150 mL of dry toluene under argon in a 250 mL Schlenk flask. The suspension was cooled to –78 °C, and a diethyl ether solution of methylolithium (1.05 mmol, 0.65 mL of a 1.6 M solution) was added dropwise with stirring. The mixture was then allowed to slowly warm to room temperature and stirred for 12 h. Solvent was removed in vacuo from the purple solution. The residue was dissolved in dry toluene and filtered under argon through deactivated silica gel ($\text{SiO}_2/\text{Cl}_2\text{SiMe}_2$). Solvent was removed in vacuo, and the residue recrystallized at –30 °C from toluene to yield 0.49 g (74%) of **11**. (Slow diffusion of pentane vapor into a saturated toluene solution of **11** gave single crystals for the X-ray crystal structure analysis.) Alternatively, complex **11** was prepared by treatment of complex **10** (300 mg, 0.41 mmol) with butadiene–magnesium (100 mg, 0.45 mmol) in toluene (30 mL). The two components were mixed with precooled toluene at –78 °C and allowed to warm to room temperature overnight to yield 137 mg (48%) of complex **11** as a violet-colored solid.

Anal. Calcd for $\text{C}_{43}\text{H}_{47}\text{N}_3\text{ClCo}$ (700.3): C, 73.76; H, 6.77; N, 6.00. Found: C, 73.40; H, 6.94; N, 5.94. ^1H NMR (d_6 -benzene): δ 9.53 (t, 1H, 6-H), 7.23 (d, 2H, 5-H, 7-H), 7.82 (d, 4H), 7.32 (t, 2H), 7.04 (t, 4H, Ph), 7.46 (t, 2H), 7.25 (d, 4H), 3.66 (sept., 4H), 1.16 (d, 24H, 2,6-diisopropylphenyl). $^{13}\text{C}\{^1\text{H}\}$ NMR (d_6 -benzene): δ 168.1 (C=N), 155.3 (C3, C8), 123.8 (C5, C7), 117.5 (C6), 140.0, 123.6, 128.3, 128.0 (ipso-, *o*-, *m*-, *p*- of Ph), 152.0, 140.9, 128.6, 127.1 (ipso-, *o*-, *m*-, *p*- of 2,4-diisopropyl-Ph), 29.3 (CHMe_2), 24.6 and 23.3 ($\text{CH}(\text{CH}_3)_2$).

X-ray crystal structure analysis of **11**: formula $\text{C}_{43}\text{H}_{47}\text{ClN}_3\text{Co}$, M = 700.22, red crystal $0.40 \times 0.30 \times 0.08 \text{ mm}^3$, a = 9.872(1) Å, b = 27.669(1) Å, c = 13.890(1) Å, β = 96.96(1)°, V = 3766.1(5) Å³, ρ_{calcd} = 1.235 g cm^{-3} , μ = 5.60 cm^{-1} , empirical absorption correction ($0.807 \leq T \leq 0.957$), Z = 4, monoclinic, space group $P2_1/n$ (No. 14), λ = 0.710 73 Å, T = 198 K, ω and φ scans, 38 470 reflections collected

($\pm h, \pm k, \pm l$), $[(\sin \theta)/\lambda] = 0.68 \text{ \AA}^{-1}$, 9330 independent ($R_{\text{int}} = 0.038$) and 7398 observed reflections [$I \geq 2\sigma(I)$], 441 refined parameters, $R = 0.039$, $wR^2 = 0.082$, max residual electron density 0.32 (-0.31) e \AA^{-3} , hydrogens calculated and refined as riding atoms.

Preparation of Complex 12:^{9a} Similarly as described above for the preparation of **10**, the bis(aryliminoethyl)pyridine Schiff base system (3.12 g, 6.45 mmol) was reacted with CoCl_2 (0.84 g, 6.45 mmol) in a total of 70 mL of *n*-butanol. Workup analogously as described above gave 3.88 g (98%) of **12** as a yellow-brown solid, that was subjected to the subsequent reduction reaction without further characterization.

Reaction of Complex 12 with "Butadiene-Magnesium": Preparation of Complex 13: A 250 mL Schlenk flask was charged with solid **12** (4.88 g, 7.92 mmol) and $\{[\text{butadiene-magnesium}] 2 \text{ THF}\}_n$ (1.94 g, 8.75 mmol). The mixture was cooled to $-78 \text{ }^\circ\text{C}$, and then precooled toluene (150 mL) was slowly added with stirring. The reaction mixture was allowed to slowly warm to room temperature and then stirred for 12 h. Solvent was removed from the purple reaction mixture in vacuo, and the residue was taken up in toluene and filtered through deactivated silica gel ($\text{SiO}_2/\text{Cl}_2\text{SiMe}_2$). Solvent was evaporated from the filtrate in vacuo, and the residue recrystallized from toluene at $-30 \text{ }^\circ\text{C}$ to give 0.92 g (56%) of **13**. (Slow crystallization from a saturated toluene solution at $-30 \text{ }^\circ\text{C}$ gave single crystals of **13** for the X-ray crystal structure analysis.) Anal. Calcd for $\text{C}_{33}\text{H}_{43}\text{N}_3\text{ClCo}$ (576.1): C, 68.80; H, 7.52; N, 7.29. Found: C, 68.50; H, 7.53; N, 7.19. $^1\text{H NMR}$ (d_6 -benzene): δ 9.53 (t, 1H, 6-H), 6.91 (d, 2H, 5-H, 7-H), 7.41 (t, 2H), 7.26 (d, 4H), 3.33 (sept., 4H, CHMe_2), 1.17 (d, 12H), 1.05 (d, 12H, $\text{CH}(\text{CH}_3)_2$ of 2,6-diisopropylphenyl), 0.05 (s, 6H, $\text{N}=\text{C}(\text{CH}_3)$). $^{13}\text{C}\{^1\text{H}\}$ NMR (d_6 -benzene): δ 167.3 ($\text{N}=\text{C}$), 152.8 (C3, C8), 125.5 (C5, C7), and 114.9 (C6), 150.9, 140.8, 127.1, 123.8 (*o*-, *ipso*-, *p*-, *m*- of 2,4-diisopropylphenyl), 29.1 (CHMe_2), 24.0 and 23.8 ($\text{CH}(\text{CH}_3)_2$), 21.2 ($\text{N}=\text{C}(\text{CH}_3)$).

X-ray crystal structure analysis of **13**: formula $\text{C}_{33}\text{H}_{43}\text{ClN}_3\text{Co}$, $M = 576.08$, red-black crystal $0.30 \times 0.20 \times 0.07 \text{ mm}^3$, $a = 8.775(1) \text{ \AA}$, $b = 22.971(1) \text{ \AA}$, $c = 15.634(1) \text{ \AA}$, $\beta = 101.20(1)^\circ$, $V = 3091.3(4) \text{ \AA}^3$, $\rho_{\text{calc}} = 1.238 \text{ g cm}^{-3}$, $\mu = 6.67 \text{ cm}^{-1}$, empirical absorption correction ($0.825 \leq T \leq 0.955$), $Z = 4$, monoclinic, space group $P2_1/n$ (No. 14), $\lambda = 0.71703 \text{ \AA}$, $T = 198 \text{ K}$, ω and φ scans, 21 505 reflections collected ($\pm h, \pm k, \pm l$), $[(\sin \theta)/\lambda] = 0.68 \text{ \AA}^{-1}$, 7772 independent ($R_{\text{int}} = 0.053$) and 4939 observed reflections [$I \geq 2\sigma(I)$], 353 refined parameters, $R = 0.050$, $wR^2 = 0.096$, max residual electron density 0.37 (-0.34) e \AA^{-3} , hydrogens calculated and refined as riding atoms.

Preparation of Complex 14: Similarly as described above for the preparation of **15**, the cobalt complex **11** (50.0 mg, 71.4 μmol) was reacted with $\text{Li}[\text{B}(\text{C}_6\text{F}_5)_4]$ (58.8 mg, 85.7 μmol) in a total of 5 mL of toluene. The deep red solution was stirred for 1 h, and subsequently pyridine (6.77 mg 85.6 μmol) was added. Workup analogously as described above gave 46.7 mg (46%) of **14** as a deep blue solid. IR (KBr): $\tilde{\nu} = 3065, 2961, 2865, 1639, 1513, 1465, 1260, 1083, 978, 800, \text{ cm}^{-1}$. MS (ESI+): $m/z = 743$. $^1\text{H NMR}$ (d_6 -benzene): δ 9.11 (t, 1H, 6-H), 7.54 (d, 4H, 5-H, 7-H), 7.31 (t, 2H), 7.15–6.96 (m, 13H), 2.60 (sept., 4H, CHMe_2), 0.69 (d, 12H), 0.67 (d, 12H, $\text{CH}(\text{CH}_3)_2$ of 2,6-diisopropylphenyl). $^{13}\text{C}\{^1\text{H}\}$ NMR (d_6 -benzene): δ 171.8 ($\text{N}=\text{C}$), 155.2 (C3, C8), 148.6, 140.5, 136.8, 129.8, 129.6, 129.5, 129.3, 128.5, 128.1, 127.9, 125.6, 125.3, 125.0 (Ar), 29.9 (CHMe_2), 23.5, 23.4 ($\text{CH}(\text{CH}_3)_2$).

Reaction of 13 with $\text{Li}[\text{B}(\text{C}_6\text{F}_5)_4]$ and Pyridine. Formation of 15: The cobalt complex **13** (100 mg, 0.40 mmol) and $\text{Li}[\text{B}(\text{C}_6\text{F}_5)_4]$ (308 mg, 0.45 mmol) were dissolved in 15 mL of toluene. The mixture was stirred for 1 h, and then dry pyridine (0.03 mL) was added. The color of the solution changed from purple to deep blue. The mixture was filtered, and the solvent was removed from the clear filtrate in vacuo. The residue was dissolved in dry bromobenzene (4 mL), and pentane vapor was allowed to slowly diffuse into the solution to give crystalline **15** after 24 h. Repeating the crystallization procedure gave single crystals of **15** suited for the X-ray crystal structure analysis. Anal.

Calcd for $\text{C}_{62}\text{H}_{48}\text{N}_4\text{BF}_{20}\text{Co}$ (1298.8): C, 57.34; H, 3.73; N, 4.31. Found: C, 56.75; H, 3.77; N, 3.74. MS (ESI+): $m/z = 619.4$ (M^+).

X-ray crystal structure analysis of **15**: formula $\text{C}_{38}\text{H}_{48}\text{N}_4\text{Co} \cdot \text{B}(\text{C}_6\text{F}_5)_4 \cdot \text{C}_6\text{H}_5\text{Br}$, $M = 1455.79$, light green crystal $0.45 \times 0.15 \times 0.03 \text{ mm}^3$, $a = 20.027(1) \text{ \AA}$, $b = 12.241(1) \text{ \AA}$, $c = 25.895(1) \text{ \AA}$, $\beta = 93.75(1)^\circ$, $V = 6334.6(7) \text{ \AA}^3$, $\rho_{\text{calc}} = 1.526 \text{ g cm}^{-3}$, $\mu = 10.07 \text{ cm}^{-1}$, empirical absorption correction ($0.660 \leq T \leq 0.970$), $Z = 4$, monoclinic, space group $P2_1/c$ (No. 14), $\lambda = 0.71073 \text{ \AA}$, $T = 198 \text{ K}$, ω and φ scans, 20 215 reflections collected ($\pm h, \pm k, \pm l$), $[(\sin \theta)/\lambda] = 0.59 \text{ \AA}^{-1}$, 11 147 independent ($R_{\text{int}} = 0.063$) and 6954 observed reflections [$I \geq 2\sigma(I)$], 866 refined parameters, $R = 0.056$, $wR^2 = 0.114$, max residual electron density 0.55 (-0.66) e \AA^{-3} , hydrogens calculated and refined as riding atoms.

Reaction of Complex 10 with Methylolithium. Preparation of Complex 16: A solution of complex **10** (300 mg, 0.41 mmol) in diethyl ether (30 mL) was cooled to $-78 \text{ }^\circ\text{C}$. Methylolithium in ether (0.77 mL, 1.6 M solution, 1.23 mmol, 3 equiv) was added dropwise with stirring. The mixture was allowed to warm to room temperature overnight and then stirred for additional 2 d. A precipitate was removed by filtration and the solvent removed in vacuo to give 252 mg (98%) of **16**. $^1\text{H NMR}$ (d_6 -benzene): δ 10.04 (t, $J_{\text{HH}} = 7.8 \text{ Hz}$, 1H, 6-H), 8.25 (pd, 4H, *o*-Ph), 8.18 (d, $J_{\text{HH}} = 7.8 \text{ Hz}$, 2H, 5-H, 7-H), 7.53 (pt, 2H, *p*-Ph), 7.48 (t, $J_{\text{HH}} = 7.9 \text{ Hz}$, 2H, Ar), 7.29 (d, $J_{\text{HH}} = 7.9 \text{ Hz}$, 4H, Ar), 6.97 (pt, 4H, *m*-Ph), 3.26 (sept., $J_{\text{HH}} = 6.8 \text{ Hz}$, 4H, CHMe_2), 1.07 (s, 3H, CoMe), 1.05 (d, $J_{\text{HH}} = 6.8 \text{ Hz}$, 12H), 0.56 (d, $J_{\text{HH}} = 6.8 \text{ Hz}$, 12H, $\text{CH}(\text{CH}_3)_2$ of 2,6-diisopropylphenyl).

Alternative Preparation of Complex 16: A solution of the complex **10** (200 mg, 0.27 mmol) in toluene (30 mL) was reacted with MeLi (0.18 mL, 1.5 M solution in ether, 0.27 mmol) at $0 \text{ }^\circ\text{C}$ for 12 h to a red brown suspension. After removal of the ether in vacuo, MeMgBr (0.43 mL, 1.9 M solution in ether, 0.81 mmol, 3 equiv) was added and the mixture was stirred for further 4 days at room temperature. The green suspension was filtered, and dioxane (30 mL) was added to the clear filtrate. The formed white precipitate was removed by filtration, and subsequently the solvent was removed in vacuo to give 144 mg (78%) of **16**. (Some dioxane was left in the product.)

Reaction of Complex 12 with Methylolithium. Preparation of Complex 17:⁷ Analogously as described above complex **12** (300 mg, 0.49 mmol) was reacted with 3 molar equiv of methylolithium in ether (0.92 mL, 1.6 M solution, 1.47 mmol) to give 250 mg (92%) of the previously described⁷ complex **17**. $^1\text{H NMR}$ (d_6 -benzene): δ 10.19 (t, $J_{\text{HH}} = 7.6 \text{ Hz}$, 1H, 6-H), 7.86 (d, $J_{\text{HH}} = 7.6 \text{ Hz}$, 2H, 5-H, 7-H), 7.49 (t, $J_{\text{HH}} = 7.7 \text{ Hz}$, 2H), 7.37 (d, $J_{\text{HH}} = 7.7 \text{ Hz}$, 4H, Ar), 3.13 (sept., $J_{\text{HH}} = 6.8 \text{ Hz}$, 4H, CHMe_2), 1.19 (d, $J_{\text{HH}} = 6.8 \text{ Hz}$, 12H), 0.62 (d, $J_{\text{HH}} = 6.8 \text{ Hz}$, 12H, $\text{CH}(\text{CH}_3)_2$ of 2,6-diisopropylphenyl), 0.58 (s, 3H, CoMe), -1.14 (s, 6H, $\text{N}=\text{CMe}$).

Preparation of Pyridine-2,6-dicarboxylic Acid Bis[2,6-diisopropylphenyl]amide (21): 2,6-Pyridinedicarbonyl dichloride (500 mg, 2.45 mmol) was dissolved in 15–20 mL of dry THF. Diisopropylaniline (924 μL , 4.90 mmol) and triethylamine (683 μL , 4.90 mmol), dried over molecular sieves (4 \AA), were added at $0 \text{ }^\circ\text{C}$. The reaction mixture was allowed to stir at room temperature for 2 h. The precipitated $\text{Et}_3\text{N} \cdot \text{HCl}$ was filtered off, and the solvent of the filtrate removed in a vacuum. The crude material was triturated with boiling hexane to provide the product as a white solid, which was dried in CH_2Cl_2 (DCM) over magnesium sulfate. Single crystals were grown from methanol at room temperature through solvent evaporation. Yield: 1.05 g, 88%, mp = $210 \text{ }^\circ\text{C}$, MS-EI (m/z) calcd = 485.3042, found = 485.3050. Anal. Calcd For $\text{C}_{31}\text{H}_{39}\text{N}_3\text{O}_2$ (485.65 g/mol): C, 76.66; H, 8.09; N, 8.65. Found: C, 76.56; H, 8.14; N, 8.75. $^1\text{H NMR}$ (d_6 -benzene): δ 9.12 (br s, 2H, NH), 9.32 (d, $J_{\text{HH}} = 7.6 \text{ Hz}$, 2H, H-3, H-5), 7.23 (t, $J_{\text{HH}} = 7.6 \text{ Hz}$, 1H, H-11), 7.13 (d, $J_{\text{HH}} = 7.6 \text{ Hz}$, 4H, H-10), 7.04 (t, $J_{\text{HH}} = 7.6 \text{ Hz}$, 1H, H-4), 3.28 (sept., $J_{\text{HH}} = 6.9 \text{ Hz}$, 4H, CH), 1.20 (d, $J_{\text{HH}} = 6.9 \text{ Hz}$, 24H, CH_3). $^{13}\text{C}\{^1\text{H}\}$ NMR (d_6 -benzene, 298 K): δ 163.0 (C-7), 149.8 (C-2, C-6), 146.9 (C-9), 140.0 (C-4), 132.2 (C-8), 129.1 (C-3, C-5), 126.2 (C-10), 124.3 (C-11), 29.9 (C-CH), 24.1 (C- CH_3).

Preparation of N^2,N^6 -Bis(2,6-diisopropylphenyl)pyridine-2,6-dicarboximide Dimethyl Ester (22): Pyridine-2,6-dicarboxylic acid bis[2,6-diisopropylphenyl] amide (**21**) (394 mg, 0.81 mmol) and trimethylxonium tetrafluoroborate (300 mg, 2.03 mmol) were suspended in DCM (20 mL) and refluxed at 55 °C for 3 days. The yellow solution was diluted with DCM and washed with a concentrated solution of sodium bicarbonate. The organic layer was dried over MgSO_4 and filtered, and all volatiles were removed to yield the crude material as a yellow oil. Extraction with pentane, filtration, and crystallization at -35 °C yield the product as a yellow crystalline powder. Yield: 287 mg, 69%, MS-EI (m/z) calcd = 513.3355, found = 513.3375. Anal. Calcd for $\text{C}_{33}\text{H}_{43}\text{N}_3\text{O}_2$ (513.70 g/mol): C, 77.15; H, 8.44; N, 8.18. Found: C, 77.14; H, 8.54; N, 8.31. ^1H NMR (d_1 -chloroform, 298 K): δ 7.36 (br s, 1H, *p*-pyridine), 7.13 (br s, 1H, *m*-pyridine), 7.03 (m, 4H, *m*-aryl), 6.97 (dd, $J_{\text{HH}} = 5.8$ Hz, 2H, *p*-aryl), 3.91 (br s, 6H, OMe), 2.88 (sept., $J_{\text{HH}} = 6.8$ Hz, 4H, CH), 1.13 (d, $J_{\text{HH}} = 6.8$ Hz, 12H, CH_3), 0.90 (d, $J_{\text{HH}} = 6.8$ Hz, 12H, CH_3). $^{13}\text{C}\{^1\text{H}\}$ NMR (d_1 -chloroform, 298 K): δ 154.0 (*o*-pyridine), 149.3 (*i*-aryl), 142.9 (*o*-aryl), 137.0 (*m*-pyridine), 136.4 (*p*-pyridine), 124.8 (*p*-aryl), 123.1 (*m*-aryl), 54.7 (br s, OMe), 28.4 (CH_3), 23.6 (CH_3), 22.6 (CH). A signal for the $\text{O}-^{13}\text{C}=\text{N}$ carbon was not observed.

X-ray crystal structure analysis of **22**: formula $\text{C}_{33}\text{H}_{43}\text{N}_3\text{O}_2$, $M = 513.70$, light yellow crystal $0.25 \times 0.2 \times 0.2$ mm 3 , $a = 27.093(1)$ Å, $b = 27.093$ Å, $c = 8.2461(3)$ Å, $\alpha = 90^\circ$, $\beta = 90^\circ$, $\gamma = 90^\circ$, $V = 6052.7(3)$ Å 3 , $\rho_{\text{calcd}} = 1.127$ g cm $^{-3}$, $\mu = 0.070$ cm $^{-1}$, $Z = 8$, tetragonal, space group $I4$, $\lambda = 0.71073$ Å, $T = 117(1)$ K, 20 962 reflections collected, 7123 independent ($R_{\text{int}} = 0.0208$), 515 refined parameters, $R = 0.0338$, $wR^2 = 0.0827$, max residual electron density 0.206 (-0.139) e Å $^{-3}$.

Preparation of Complex 23: The ligand (**22**) (300 mg, 0.58 mmol) and iron(II) chloride (74 mg, 0.58 mmol) were combined in THF (40 mL), and the dark red solution was stirred overnight until no iron salt was detectable anymore. All volatiles were removed in a vacuum to give the product as light pink powder. Red single crystals were grown from hot toluene by cooling to room temperature overnight. Yield: 189 mg, 51%, Anal. Calcd for $\text{C}_{33}\text{H}_{43}\text{Cl}_2\text{FeN}_3\text{O}_2$ (640.45 g/mol): C, 61.88; H, 6.77; N, 6.56. Found: C, 62.31; H, 6.69; N, 6.78.

X-ray crystal structure analysis of **23**: formula $\text{C}_{33}\text{H}_{43}\text{Cl}_2\text{FeN}_3\text{O}_2$, $M = 732.59$, red crystal $0.25 \times 0.2 \times 0.1$ mm 3 , $a = 11.5856(5)$ Å, $b = 18.9039(10)$ Å, $c = 34.7620(16)$ Å, $\alpha = 90^\circ$, $\beta = 90^\circ$, $\gamma = 90^\circ$, $V = 7613.3(6)$ Å 3 , $\rho_{\text{calcd}} = 1.278$ g cm $^{-3}$, $\mu = 0.574$ mm $^{-1}$, $Z = 8$, orthorhombic, space group $Pbca$, $\lambda = 0.71073$ Å, $T = 117(1)$ K, 39 192 reflections collected, 8912 independent ($R_{\text{int}} = 0.0334$), 456 refined parameters, $R = 0.0572$, $wR^2 = 0.1449$, max residual electron density 1.627 (-0.730) e Å $^{-3}$.

Preparation of Complex 24: The ligand (**22**) (300 mg, 0.58 mmol) and cobalt(II) chloride (76 mg, 0.58 mmol) were combined in THF (40 mL), and the green solution was stirred for several hours until no cobalt salt was detectable anymore. The reaction volume was reduced in a vacuum and pentane was layered onto the solution. Crystallization took place at -35 °C, and the resulting green solid was filtered and dried in vacuo (315 mg, 84%). Green single crystals were grown from THF by pentane diffusion at -35 °C. Anal. Calcd for $\text{C}_{33}\text{H}_{43}\text{Cl}_2\text{CoN}_3\text{O}_2$ (643.5): C, 61.59; H, 6.73; N, 6.53. Found: C, 61.90; H, 6.52; N, 6.04.

X-ray crystal structure analysis of **24**: formula $\text{C}_{33}\text{H}_{43}\text{Cl}_2\text{CoN}_3\text{O}_{3.50}$, $M = 751.69$, green crystal $0.2 \times 0.1 \times 0.1$ mm 3 , $a = 35.520(3)$ Å, $b = 11.5844(10)$ Å, $c = 18.7071(16)$ Å, $\alpha = 90^\circ$, $\beta = 90^\circ$, $\gamma = 90^\circ$, $V = 7697.6(11)$ Å 3 , $\rho_{\text{calcd}} = 1.297$ g cm $^{-3}$, $\mu = 0.626$ mm $^{-1}$, $Z = 8$, orthorhombic, space group $Pbcn$, $\lambda = 0.71073$ Å, $T = 117(1)$ K, 25626 reflections collected, 4545 independent ($R_{\text{int}} = 0.0638$), 460 refined parameters, $R = 0.0566$, $wR^2 = 0.1208$, max residual electron density 0.611 (-0.466) e Å $^{-3}$.

Preparation of Complex 25/26: Complex **24** (800 mg, 1.24 mmol) was dissolved in toluene (80 mL), and methyl lithium (1.71 mL, 1.6 M in diethyl ether, 2.48 mmol) was added to the green suspension under

nitrogen. The solution turned purple and was allowed to stir at room temperature for 12 h. The volume was reduced in a vacuum to remove diethyl ether and filtered over Celite. All volatiles were removed in a vacuum to give the product as a purple crystalline solid, consisting of an isomeric mixture (600 mg, 82%). Single crystals of the $\text{N}\wedge\text{N}\wedge\text{N}$ -isomer **26** were grown from toluene by pentane diffusion at room temperature. Anal. Calcd for $\text{C}_{34}\text{H}_{46}\text{CoN}_3\text{O}_2$ (588.7): C, 69.49; H, 7.89; N, 7.15. Found: C, 69.28; H, 7.54; N, 6.62. ^1H NMR (d_6 -benzene): δ 10.48 (t, 1H, $^3J_{\text{HH}} = 7.7$ Hz, *para*-pyridine-Ph), 7.86 (d, 2H, $^3J_{\text{HH}} = 7.7$ Hz, *meta*-pyridine-Ph), 7.49 (dd, 2H, $^3J_{\text{HH}} = 7.4$ Hz, *para*-aniline-Ph), 7.41 (d, 4H, *meta*-aniline-Ph), 3.69 (s, 6H, OCH $_3$), 3.33 (p, 4H, $^3J_{\text{HH}} = 6.8$ Hz, CH), 1.36 (d, 12 H, $^3J_{\text{HH}} = 6.8$ Hz, CH $_3$), 0.75 (d, 12H, $^3J_{\text{HH}} = 6.8$ Hz, CH $_3$), 0.34 (s, 3H, CoCH $_3$). $^{13}\text{C}\{^1\text{H}\}$ NMR (d_6 -benzene): δ 166.8 (COMe), 150.5 (*para*-pyridine-C), 147.0 (*ortho*-aniline-C), 142.2 (*ortho*-pyridine-C), 126.9 (*meta*-pyridine-C), 126.0 (*para*-aniline-C), 124.0 (*meta*-aniline-C), 113.7 (*ipso*-aniline-C), 50.9 (OCH $_3$), 29.2 (CH), 24.6 (CH $_3$), 23.7 (CH $_3$), 14.6 (CoCH $_3$).

[Isomeric mixture: ^1H NMR (d_6 -benzene): δ 10.48 (t, 1H, $^3J_{\text{HH}} = 7.7$ Hz, *para*-pyridine-Ph), 10.31 (t, 1H, $^3J_{\text{HH}} = 7.5$ Hz, *para*-pyridine-Ph), 10.20 (t, 1H, $^3J_{\text{HH}} = 7.5$ Hz, *para*-pyridine-Ph), 8.21 (d, 2H, $^3J_{\text{HH}} = 7.5$ Hz, *meta*-pyridine-Ph), 7.64 to 6.96 (m, 22H, aniline- and pyridine-Ph), 3.88 (s, 9H, OCH $_3$), 3.69 (s, 9H, OCH $_3$), 3.33 (p, 4H, $^3J_{\text{HH}} = 6.8$ Hz, CH), 3.19 (m, 8H, CH), 1.36 (d, 18 H, $^3J_{\text{HH}} = 6.8$ Hz, CH $_3$), 1.19 (m, 18 H, CH $_3$), 0.86 (d, 6 H, $^3J_{\text{HH}} = 6.8$ Hz, CH $_3$), 0.75 (d, 12 H, $^3J_{\text{HH}} = 6.8$ Hz, CH $_3$), 0.64 (d, 12 H, $^3J_{\text{HH}} = 6.8$ Hz, CH $_3$), 0.60 (s, 3H, CoMe), 0.54 (d, 6 H, $^3J_{\text{HH}} = 6.8$ Hz, CH $_3$), 0.53 (s, 3H, CoMe), 0.34 (s, 3H, CoMe).]

X-ray crystal structure analysis of **26**: formula $\text{C}_{34}\text{H}_{46}\text{CoN}_3\text{O}_2$, $M = 587.67$, red crystal $0.2 \times 0.2 \times 0.15$ mm 3 , $a = 11.7149(9)$ Å, $b = 13.5659(10)$ Å, $c = 20.8201(16)$ Å, $\alpha = 90^\circ$, $\beta = 105.229(2)^\circ$, $\gamma = 90^\circ$, $V = 3192.6(4)$ Å 3 , $\rho_{\text{calcd}} = 1.223$ g cm $^{-3}$, $\mu = 0.571$ mm $^{-1}$, $Z = 4$, monoclinic, space group $P2(1)/n$, $\lambda = 0.71073$ Å, $T = 117(1)$ K, 20 654 reflections collected, 7109 independent ($R_{\text{int}} = 0.0309$), 545 refined parameters, $R = 0.0390$, $wR^2 = 0.0950$, max residual electron density 0.444 (-0.239) e Å $^{-3}$.

Generation of Complex 27: Complex **25/26** (26 mg, 0.044 mmol) was dissolved in toluene (3 mL), and $\text{B}(\text{C}_6\text{F}_5)_3$ (113 mg, 0.22 mmol) in toluene (3 mL) was added. The purple reaction mixture turned blue immediately. The reaction was stirred for 5 min and filtered over Celite. Crystallization from chlorobenzene with pentane diffusion at room temperature provided the product as brown crystals.

X-ray crystal structure analysis of **27**: formula $\text{C}_{52}\text{H}_{46}\text{BCoF}_{15}\text{N}_3\text{O}_2$, $M = 1099.66$, brown crystal $0.25 \times 0.2 \times 0.15$ mm, $a = 18.2816(7)$, $b = 13.9935(5)$, $c = 18.7573(7)$ Å, $\alpha = 90^\circ$, $\beta = 96.3120(10)^\circ$, $\gamma = 90^\circ$, $V = 4769.5(3)$ Å 3 , $\rho_{\text{calc}} = 1.531$ g cm $^{-3}$, $\mu = 0.465$ mm $^{-1}$, $Z = 4$, monoclinic, space group $P2(1)/c$, $\lambda = 0.71073$ Å, $T = 117(1)$ K, 26459 reflections collected, 9376 independent ($R_{\text{int}} = 0.0306$), 690 refined parameters, $R = 0.0456$, $wR^2 = 0.1112$, max. residual electron density 0.361 (-0.673) e Å $^{-3}$.

Ethene Polymerization Reactions, General Procedure: In an inert atmosphere the respective complex was reacted with the activator in 40 mL of toluene in a 100 mL Schlenk flask. The flask was evacuated and purged with ethene (2 bar) at room temperature. The reaction mixture was stirred under a constant pressure of 2 bar ethene for 0.5 h at room temperature. Then the ethene pressure was released, and the reaction was quenched with methanol (20 mL). The obtained polyethylene was collected and consecutively washed with acetone, water, and THF. The remaining polymer was stirred with THF (20 mL) over 8 h to remove remaining impurities. The polymer was then dried overnight in vacuo at 50 °C.

To control the polymerization equipment, every time before the polymerization a standard polymerization reaction was carried out following the general procedure described above: Cp_2ZrMe_2 (5 mg, 0.02 mmol), $\text{B}(\text{C}_6\text{F}_5)_3$ (10 mg, 0.02 mmol) in 40 mL of toluene.

The polymer was characterized by C,H elemental analysis, DSC, and ^{13}C NMR spectroscopy; the obtained polymer is linear polyethylene.

Two polymerization reactions starting from **17** (R = Ph) [each 50 mg **17** / 61.7 mg Li[B(C₆F₅)₄]: 1.701 g; 2.217 g PE] produced polyethylene with an average activity of $a = 22$ g(PE) mmol(cat.)⁻¹ h⁻¹ bar⁻¹. Two experiments starting from **16** [each 50.0 mg of **16**/50.40 mg of Li[B(C₆F₅)₄]: 2.500 g; 2.340 g] produced polyethylene with a average activity of $a = 33$ g(PE) mmol(cat.)⁻¹ h⁻¹ bar⁻¹.

For compound **24**, **25/26**, and **27**, the respective cobalt compound (6 mg) was reacted with Li[B(C₆F₅)₄] (34 mg), MAO, or MAO/BF₃ if appropriate in 30 mL of toluene, and the reactor was purged with 100 psi (6.8 bar) of ethene. Polymerization reactions were run for 20 min at room temperature. The ethene pressure was released, and the reaction was quenched with methanol. The obtained polyethylene was washed with acetone and dried in a vacuum. The polymer was characterized by DSC and GPC. The obtained polymer is linear polyethylene. Representative polymerization reactions for the isomeric mixture (**25/26**) gave activities ranging from 28 to 38 g(PE) mmol(**25/26**)⁻¹ h⁻¹ bar⁻¹. A single experiment with the isomerically pure crystalline complex **26** activated with Li[B(C₆F₅)₄] under the same conditions gave a slightly lower activity ($a = 21$ g(PE) mmol(**26**)⁻¹ h⁻¹ bar⁻¹). No

polyethylene was obtained with compound **27**. Control experiments using just Li[B(C₆F₅)₄] (1.00 g) or the complexes **16** and **17** or **25/26** without activator components under otherwise analogous conditions produced no polyethylene.

Acknowledgment. Financial support from the Deutsche Forschungsgemeinschaft and the Fonds der Chemischen Industrie is gratefully acknowledged. G.C.B. and J.-C.W. are grateful to the DOE (DE-FG03098ER 14910) for financial support.

Supporting Information Available: CIF files giving details of the X-ray crystal structure analysis (**8**, **9**, **10**, **11**, **13**, **15**, **22**, **23**, **24**, **26**, and **27**) and text giving additional information about the polymerization experiments, spectroscopic data, and details of the X-ray crystal structure determinations. This material is available free of charge via the Internet at <http://pubs.acs.org>.

JA052129K